

**DESIGN AND SIMULATION OF ZNO-BASED DIELECTRIC  
OPTICAL ANTENNAS AND INVESTIGATION OF THEIR FAR-  
FIELD RADIATION USING FDTD METHOD**

by

Chaitanya Sai Raju Venna

A Research Study Submitted in Partial Fulfillment of the Requirements for the Degree  
of Master of Engineering in Nanotechnology

Examination Committee: Dr. Tanujjal Bora (Chairperson)  
Dr. Attaphongse Taparugssanagorn  
Dr. Waleed Mohammed

Nationality: Indian

Previous Degree: Bachelor of Technology in Electronics and  
Telecommunications Engineering,  
Jawaharlal Nehru Technological University,  
Hyderabad, Telangana, India

Scholarship Donor: AIT Fellowship

Asian Institute of Technology  
School of Engineering and Technology  
Thailand  
May 2021

## **AUTHOR'S DECLARATION**

I, Chaitanya Sai Raju Venna, declare that the research work carried out for this Research work which was in accordance with the regulations of the Asian Institute of Technology. The work presented in it are my own and has been generated by me as the result of my own original research, and if external sources were used, such sources have been cited. It is original and has not been submitted to any other institution to obtain another degree or qualification. This is a true copy of the Research study, including final revisions.

Date: 11/05/2021

Name: Chaitanya Sai Raju Venna

Signature:

## ACKNOWLEDGMENTS

First of all, I would like to express my heartiest gratitude to my advisor Dr. Tanujjal Bora for his continuous guidance, suggestion and resource he provided throughout my research study. It was a great privilege to work and study under his guidance. I would like to take this opportunity to express my sincere gratitude to Dr. Waleed Mohammed for helping me in my research study. I would like to thank Dr. Attaphongse Taparugssanagorn for showing interest on my research study and being part of the research committee.

I would like to thank all fellow members of Center of Excellence in Nanotechnology. I would like to acknowledge Asian Institute of Technology for granting me AIT fellowship.

I revere the support extended with love, by my beloved father Late Mr. Venna Muralidhara Rao and mother Mrs. Venna Vijaya Lakshmi for whose financial support, blessings and sacrifices made it possible for me to complete this research.

Lastly, I would like to thank all my fellow members of Center of Excellence in Nanotechnology. I give my sincere gratitude to my classmates and seniors for their continuous help, support and encouragement. I would like to thank Mr. Kunal Sharma for helping and assisting in learning the software's which are required to complete my research.

## **ABSTRACT**

Optical antennas are one of the emerging concepts in the field of optical physics. The purpose of an antenna is to convert energy of free propagating radiation to localized energy and vice versa. Such antennas are most promising at nanoscale, operating at optical frequencies, called as Optical Nano-Antennas. Optical nano-antennas typically utilize the unique morphological and optical properties of nanostructured materials, which behave as strongly coupled plasmas at optical frequencies. In this research, we conducted a theoretical study on optical nanoantenna and investigation of radiation patterns using FDTD analysis. This work involves the optical nanoantenna which exhibit high scattering which can be used to control the light propagation across the surface. an organised analysis of single and periodic array of optical nanoantenna through air dielectric is done. The scattering calculations shows high forward directivity of different nanoantenna elements.

# CONTENTS

	<b>Page</b>
<b>ACKNOWLEDGMENTS</b>	<b>III</b>
<b>ABSTRACT</b>	<b>IV</b>
<b>LIST OF TABLES</b>	<b>VII</b>
<b>LIST OF FIGURES</b>	<b>VIII</b>
<b>LIST OF ABBREVIATIONS</b>	<b>XI</b>
<b>CHAPTER 1 INTRODUCTION</b>	<b>1</b>
1.1 Background	1
1.2 Finite Difference Time Domain (FDTD) Method	2
1.3 Problem Statement	2
1.4 Objectives	3
1.5 Scope of the Study	3
<b>CHAPTER 2 LITERATURE REVIEW</b>	<b>4</b>
2.1 Concept of Optical Antenna	4
2.2 Types of Optical Antennas	4
2.2.1 Metallic Nano-Antennas	4
2.2.1 Dielectric Nano-Antennas	5
2.2.2 Non-linear Optical Antennas	7
2.3 Nanoparticle Antennas in COMSOL	9
2.4 Tuneable Nano Antenna	12
2.4.1 Boundary Conditions	13
2.4.2 The Novel Design of Nano Antenna	13
2.5 Modelling of Nanoantenna Arrays in COMSOL Multiphysics	14
2.6 Photoconductive Antenna (PCA) Using Optical Antenna Array of ZnO Nanorods	16
2.6.1 Device Structure and Design	17
<b>CHAPTER 3 METHODOLOGY</b>	<b>20</b>
3.1 Material Selection	20
3.2 Construction of Optical Nanoantenna	21

	<b>Page</b>
3.2.1 Model Setup	21
3.2.2 Meshing ...	23
3.2.3 Solving ....	24
3.2.4 Cross Section Calculations	26
3.2.5 Far Field Radiation Calculations	27
3.2.6 Post Processing	27
3.3 Construction of Array of Nanoantenna	29
<b>CHAPTER 4 RESULTS AND DISCUSSION</b>	<b>34</b>
4.1 Simulation Results of Single ZnO Nanorod Scattering and Radiation Patterns	34
4.2 Simulation and Modelling Results of Nanorod Array Scattering and Radiation Patterns	35
4.3 Simulation Results of the Effects of Size, Spacing between the Elements in Array, and Angle of Incidence of Wave Propagation of Array on Scattering and Radiation patterns	37
4.3.1 Effect of Change in Size of the Single Nanoantenna element	37
4.3.2 Effect of Change in Spacing Between the Array of Nanoantenna Element on the Scattering and Radiation Pattern	39
4.3.3 Effect of Change in Angle of Incidence of Wave Propagation on Scattering and Radiation Pattern	42
<b>CHAPTER 5 CONCLUSION AND RECOMMENDATIONS</b>	<b>47</b>
<b>REFERENCES</b>	<b>48</b>

## LIST OF TABLES

<b>Tables</b>	<b>Page</b>
Table 3.1 Material Properties of ZnO Nanoantenna in COMSOL	21

## LIST OF FIGURES

<b>Figures</b>	<b>Page</b>
Figure 2.1 Main Types of Plasmonic Nano-Antennas (Kausar Et Al., 2015)	5
Figure 2.2 Simulation of Electric Field Distribution Dielectric Microsphere (A E Krasnok Et Al., 2013)	6
Figure 2.3 Huygens Element (Filonov et al., 2012); (A E Krasnok et al., 2013).	7
Figure 2.4 Totally Dielectric Nonlinear Optical Metallic Dielectric Nano Dimer(Noskov et al., 2012)	7
Figure 2.5 Nonlinear Optical Metallic Dielectric Nano Dimer (Noskov Et Al., 2012).	8
Figure 2.6 Design Of A Nonlinear Optical Dipole (Large Et Al., 2010)	9
Figure 2.7 Far Field Scattering Cross Section of a Silver Cross as a Function of Wavelength (Djalalian-Assl Et Al., 2011)	10
Figure 2.8 The Scattering Far Field Radiation Pattern (Djalalian-Assl Et Al., 2011)	10
Figure 2.9 The Electric Field At Resonance On The Surface Of Nanoparticle, Where Red Denoted Maximum Value (Djalalian-Assl Et Al., 2011)	11
Figure 2.10 Slot Antenna With Surface Corrugations To Control Radiation (Djalalian-Assl Et Al., 2011)	11
Figure 2.11 Nano Antenna Structure (Beheshti Asl Et Al., 2019)	12
Figure 2.12 Piezoelectric Layer Between Gold Bowtie Nano Antenna And Silicon Dioxide Substrate For Tuning (Beheshti Asl Et Al., 2019)	12
Figure 2.13 The Far Field Pattern For Nano Antenna With A Gap Between 100 And 800 Nm At 193 Thz (Beheshti Asl Et Al., 2019)	13
Figure 2.14 Effect Of Changing The Geometric Of Added Nanoparticle On The Pattern Of The Nano-Antenna Simulated At 193 Thz (Beheshti Asl Et Al., 2019)	14
Figure 2.15 Unit Cell Of Nanoantenna Array (Liu Et Al., 2009)	15
Figure 2.16 The Structure Of Nanoantenna In COMSOL (Liu Et Al., 2009).	15



<b>Figures</b>	<b>Page</b>
Figure 2.17 The Reflectance And Transmittance Spectra Extracted From COMSOL, And SHA (Liu Et Al., 2009)	16
Figure 2.18 Schematic Proposed PCA In 3-D View (Bashirpour Et Al., 2019)	16
Figure 2.19 Schematic Diagram Of PCA In Front View (Bashirpour Et Al., 2019)	17
Figure 2.20 Reflections Of PCA With And Without ARC (Bashirpour Et Al., 2019)	18
Figure 2.21 Simulated Magnetic Field Distribution Of Regular PCA Without And With Zno Nrs (Bashirpour Et Al., 2019)	18
Figure 2.22 The Electric Field Distribution Of Zno Nanorods (Bashirpour Et Al., 2019)	19
Figure 3.1 Geometry of The Model Designed in COMSOL Multiphysics	22
Figure 3.2 Simulation Mechanism of Single Zno Rod	22
Figure 3.3 Meshed Geometry of The Model.	24
Figure 3.4 Parametric Sweep in Settings	28
Figure 3.5 Postprocessing View of The Model	29
Figure 3.6 Geometry of Nanoantenna Array	29
Figure 3.7 Meshed Geometry of Nanoantenna Array	30
Figure 3.8 Geometry of Single Nanoantenna With Length 300nm	31
Figure 3.9 Geometry of Single Nanoantenna with Length 1200nm	31
Figure 3.10 Geometry of 1*5 Array of Nanoantenna Element with Spacing of 50 nm	32
Figure 3.11 Geometry Of 1*5 Array of Nanoantenna Element with Spacing of 200 nm	32
Figure 3.12 Simulation Mechanism of Array of ZnO Nanorods	33
Figure 4.1 Scattering Cross Section of The Single Nanoantenna Element	34
Figure 4.2 Far Field Radiation Pattern of Single Nanoantenna Rod at Wavelength 300nm – 700nm	35
Figure 4.3 Scattering Cross Section f 1*5 Array of Nanoantenna Element	36
Figure 4.4 Far Field Radiation Patter Of 1*5 Array of Nanoantenna Element at 300nm -700nm Wavelengths	36

<b>Figures</b>	<b>Page</b>
Figure 4.5 Scattering Crosssection Of Single Nanoantenna With Length 300nm	37
Figure 4.6 Far Field Radiation Pattern for Single Nanoantenna Element with Length 300nm	38
Figure 4.7 Scattering Crosssection Of Single Nanoantenna With Length 1200nm	38
Figure 4.8 Far Field Radiation Pattern for Single Nanoantenna Element with Length 1200nm	39
Figure 4.9 Scattering Cross Section Of 1*5 Array of Nanoantenna Element with Spacing of 50 nm	40
Figure 4.10 Far Field Radiation Pattern Of 1*5 Array of Nanoantenna Element with Spacing Of 50nm	40
Figure 4.11 Scattering Cross Section of 1*5 Array of Nanoantenna Element with Spacing of 200 nm	41
Figure 4.12 Far Field Radiation Pattern of 1*5 Array of Nanoantenna Element with Spacing of 200nm	41
Figure 4.13 Scattering Cross Section Of 1*5 Array of Nanoantenna Element with Different Angle of Incidences	42
Figure 4.14 Far Field Radiation Pattern Of 1*5 Array with Angle of Incidence, Theta=15°	43
Figure 4.15 Far Field Radiation Pattern Of 1*5 Array with Angle of Incidence, Theta=30°	43
Figure 4.16 Far Field Radiation Pattern of 1*5 Array with Angle of Incidence, Theta =45°	44
Figure 4.17 Far Field Radiation Pattern of 1*5 Array with Angle of Incidence, Theta =60°	44
Figure 4.18 Far Field Radiation Pattern of 1*5 Array with Angle of Incidence, Theta =75°	45
Figure 4.19 Far Field Radiation Pattern of 1*5 Array with Angle of Incidence, Theta =90°	45

## LIST OF ABBREVIATIONS

FDTD	= Finite Definite Time Domain
OA	= Optical Antenna
ARC	= Anti Reflection Coating
PCA	= Photo Conductive Antenna
PML	= Perfectly Matched Layer
ZnO	= Zinc Monoxide
TiO <sub>2</sub>	= Titanium Dioxide

# CHAPTER 1

## INTRODUCTION

### 1.1 Background

In optics, propagating radiation through lenses, prisms and different diffractive elements from light are controlled by waves. This type of control depends on the electromagnetic fields. Conversely, microwave and radio waves use antennas to control electromagnetic fields, controlling them on sub wavelength and interfacing efficiently between propagating field and restricted fields (Kausar et al., 2015).

In present generation technologies like cellular phones and televisions antennas plays a key role in enabling the technology for the devices using electromagnetic waves in radio wave and microwave frequencies. In recent studies, the researchers in nano optics and plasmonic has intensified their research in the new field of optical antennas and their main focus is, how to interpret radiowave and microwave theory in optical frequencies spectrum (Alexander E. Krasnok et al., 2012).

Recent studies and advancements in the field of nanotechnology and optical science have led to the novel designs in antennas. The antennas which are operating at optical frequencies at nano scale are called as optical nano-antennas. Nano antenna can improve the interactions of light and matter and can provide the strong coupling between far field scattering and local sources at nanoscale (Balanis, 2005).

Nano-antennas are usually used for converting electric energy into propagating wave energy and vice versa (Kausar et al., 2015). During past years, the rapid development in wireless devices have a huge demand for devices that can operate at different frequencies. The devices like Bluetooth (2400 to 2483.5 MHz), wireless local network (standard range is 802.11), mobile devices, satellite devices require very small apparatus to receive and send information (Novotny & Van Hulst, 2011). Due to this, extensive research on the designs for RF and microwave frequency applications are started.

Optical nano-antennas have more prospects, and the most important features of optical nano-antennas are described as follows

1. Optical antennas are point detectors which secure the space of almost square of the wavelength (Alda et al., 2005).
2. They are popularly known as polarization sensitive sensors like RF sensors.
3. They are used for tuning to a wavelength spectrum. At optical frequencies, the metallic structures have a lossy character and as a result, the resonance are likely to be widened, which possibly limits the tuning ability (Codreanu & Boreman, 2002).
4. They are direction sensible to metallic structures and addition of peripheral optical devices (González et al., 2002).

## **1.2 Finite Difference Time Domain (FDTD) Method**

This method is used for computational of electrodynamics. In a simulation FDTD method can canvas a wide array of frequencies and non-linear materials are computed in general process. Before this method were mainly derived to solve the macroscopic engineering problems. However, in the recent times, this method can be used to solve at molecular level.

The problems with electromagnetic waves with their materials are dealt using FDTD method. In this method, Maxwell's equation is used for computation. By that equation, the electric field  $E$  and magnetic field  $H$  are determined at every point within the computational domain. Materials of each cell in the model should be specified. The materials can be of free space, metal or dielectric. the physical constants like permeability, permittivity, and conductivity of the material should be specified. Scattered radiation fields can be obtained by computing electromagnetic fields through FDTD method.

## **1.3 Problem Statement**

The performance of the optical devices can be limited due to the unwanted reflections from surfaces. Antireflection (AR) coatings are used to suppress such losses which reduces the Fresnel reflections of electromagnetic wave interaction with a surface. The purpose of AR coating layer is usually to achieve an optimum reflection reduction at certain frequency and incidence angle. The main constraint of AR coating is that there is no second chance for a reflected light to incident on the surface. Due to this,

nanoantenna layer which are made up of rods like structure is very useful to minimize the reflective losses.

In optical nanoantenna's, spherical nano antenna made of metals are mostly used antenna to examine the polarization, radiation pattern, directivity, and low energy conversion to THz. Despite number of advantages of metallic nanoantenna's, such antennas have large dissipative losses which resulting in low radiation efficiency and due to the aspect ratio of the spherical structure of spherical antenna, the efficiency of the electric field is limited. To overcome such limitations, we propose semiconductor based nanorod shaped antenna to enhance the radiation efficiency.

#### **1.4 Objectives**

The objectives of this research work are:

- i. Construct and model a single element optical nano-antenna using semiconductor material and study its radiation pattern.
- ii. Extend the single element nano-antenna into an array of optical nano-antennas and simulate the radiation pattern.
- iii. Investigate the effects of nano-antenna element size, spacing between the Array elements, and angle of incidence of wave propagation on the radiation pattern.

#### **1.5 Scope of the Study**

The main focus of this research work is to analyse the light propagation properties of ZnO nanorods and establish a system to control the light propagation. In this approach, we try to enhance the scattering of the light by organized analysis of single and periodic nanorods through air dielectric which shows the light scattering properties to and from a dielectric. We will analyse the effect of aspect ratio, spacing between the rods in an array, and angle of incidence of wave propagation on the scattering of the light of the dielectric nanorods.

## **CHAPTER 2**

### **LITERATURE REVIEW**

#### **2.1 Concept of Optical Antenna**

In Nano scale structures, the optical antennas consisting of interacting metallic particles with electromagnetic waves at optical frequency. The functioning of optical antennas is like Rf antennas in receiving and transmitting propagated radiation in free space. Optical antennas capture the free space electromagnetic wave and focus light energy into their high field beyond their diffraction limit. The outgoing radiation pattern from electromagnetic wave is built in metallic structure. Typically, the antenna size and design are scaled within the wavelength and it can be detected at a fraction of the wavelength.

#### **2.2 Types of Optical Antennas**

There are different types of optical antennas, namely:

1. Metallic nano-antennas
2. Dielectric nano-antennas
3. Nonlinear optical nano-antennas

##### **2.2.1 *Metallic Nano-Antennas***

The metallic nanoparticles are first used by Edward Hutchinson Synge in the field of optics in the year 1928. John Wessel reveal that a metallic nanoparticle acts as an antenna in 1985. He said that in optical devices it can surpass the diffraction resolution and resolving power up to 1 nm in the presence of a single plasmonic particle. Such antennas are called as monopoles. The strength of gap between two or more nanoparticles is higher than the area of the extended nanoparticle.

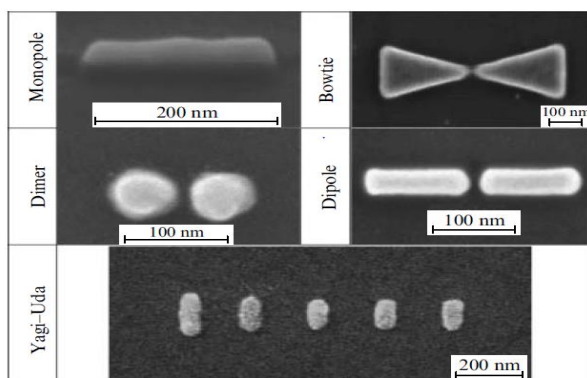
The energy is confined to smaller scales in that gap. The metal of the nanoparticle which we use, derives electric field of the gap between the particles. Electric field can be varied with construction of particle, gap width, particle radius within the gap. These parameters help in frequency positioning and amplitude at which the maximum efficiency of the field occurs (A E Krasnok et al., 2013) (Wessel, 1985).

There are different types of metallic nano-antennas:

- Plasmonic monopole - A single metallic Nano particle which has the ability to enhance the electromagnetic field capable of operating as receiving antenna upon excitation of Plasmon resonance at different order is called plasmonic monopole antenna(A E Krasnok et al., 2013; Novotny & Van Hulst, 2011).
- Plasmonic dipole - The antenna is mostly based on the field intensity of the gap between two metallic nanoparticles. There are two types of nano antennas, dipole antenna and bowtie antenna(AI & Engheta, 2008)
- Yagi Uda - Yagi Uda antennas are the oldest type of antennas which are well known in the world and they are the standard antennas at radio wave frequency owing a probability to narrow its directivity by adjusting its elements(Noskov et al., 2012).

**Figure 2.1**

*Main Types Of Plasmonic Nano-Antennas (Kausar et al., 2015)*



### **2.2.1 Dielectric Nano-Antennas**

In recent years, the optical response of the dielectric and semiconducting particles has laid a path for novel nanoantenna designs. Unlike metallic nano-antenna, Dielectric nano-antennas are fabricated by optical transparent materials which are opaque materials which exhibit plasmonic properties in the optical range. In dielectric antennas, most of the works are based on spherical particles and few of them are nanorods and nano disks (AI & Engheta, 2008; A E Krasnok et al., 2013).

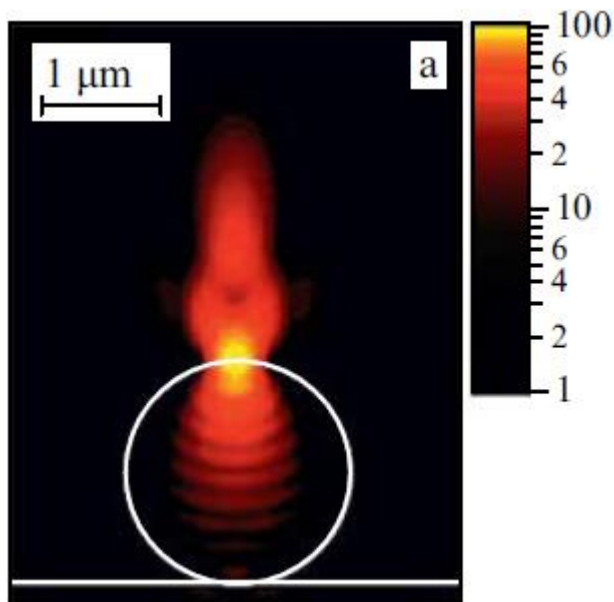


There are different types in dielectric antennas:

- **Whispering gallery antennas** - The electrodynamics of dielectrics microspheres in the form of eigenmodes called as whispering gallery modes. Due to their large radiation aperture of whispering gallery antennas involves microspheres for good directional capabilities. The main limitation of such an antenna is spontaneous relaxation rate of emitter (Filonov et al., 2012; A E Krasnok et al., 2013).

**Figure 2.2**

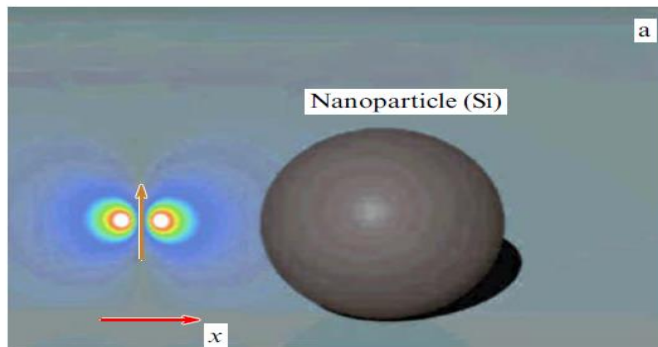
*Simulation Of Electric Field Distribution Dielectric Microsphere (A E Krasnok et al., 2013)*



- **Huygens element** – it is a type of dielectric particle which has high permittivity due to which it has the resonance in magnetic and electric at visible frequency. Depending on the size of the material and particle at certain frequencies, the electric and magnetic dipoles are equal to each other (Filonov et al., 2012; A E Krasnok et al., 2013).

**Figure 2.3**

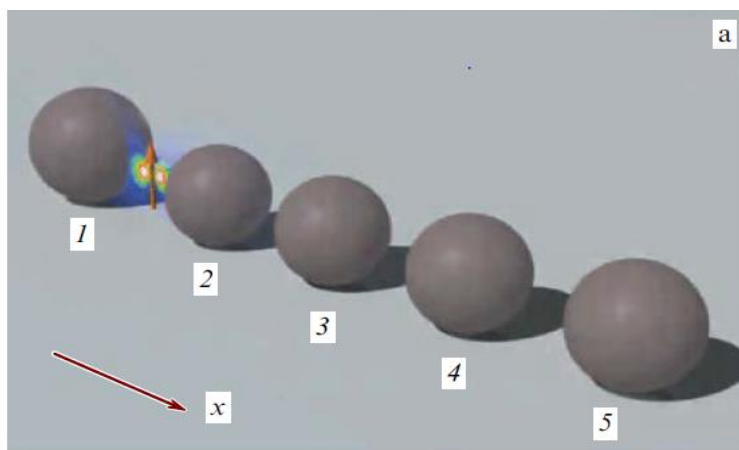
*Huygens Element* (Filonov et al., 2012; A E Krasnok et al., 2013).



- **Dielectric Yagi Uda antenna** - The concept of Huygens element is completely used for the developing dielectric Yagi Uda antenna. For this antenna, the same size nanoparticles of dielectric are added in the system to illustrate. With this type of antenna, the directivity of the radiation pattern is improved (Filonov et al., 2012)

**Figure 2.4**

*Totally Dielectric Nonlinear Optical Metallic Dielectric Nano Dimer* (Noskov et al., 2012)



### 2.2.2 Non-linear Optical Antennas

The development of nanoantennas based devices indicating the possibility of controlling the attributes such as bandwidth, field confinement. Such a specification follows in any case from the assembling nano antennas and their arrays filled with the resulting errors,

for example, India nanoantennas bit working bandwidth are running out of emitter radiating frequency. Second, the nanoantenna operations may vary in time(A E Krasnok et al., 2013). Finally, the specifications of nanoantennas allows the improvement of different nano devices such as optical switches enabling the working frequently from radiation spectrum with more complex system of stationary states(Noskov et al., 2012).

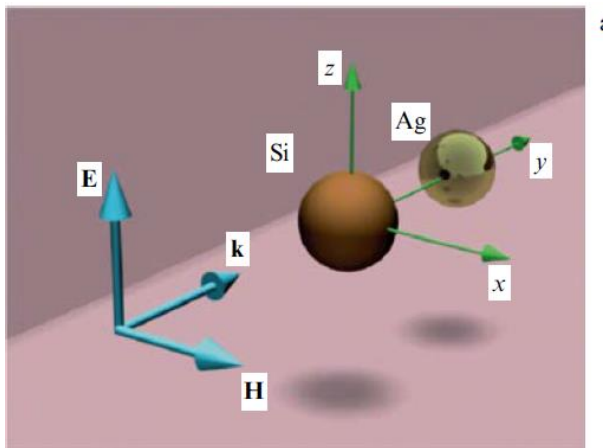
The receiving antennas provide great chances for controlling position of detectors and cross section absorption with their width. Nano-antennas must be active devices. We know that they are very small and are in optical frequency range, the most sensible method for modelling of nanoantennas is to introduce non-linearity into their process.

They are two types of non-linearity they are:

- **Non-linear optical response in metal** - The application of non-linear optical feedback of plasmonic nano elements expanding capability of photonics. in plasmonic nano particles the direction of radiation pattern can be controlled by shifting the dipole moment to the external field strength (Noskov et al., 2012).

**Figure 2.5**

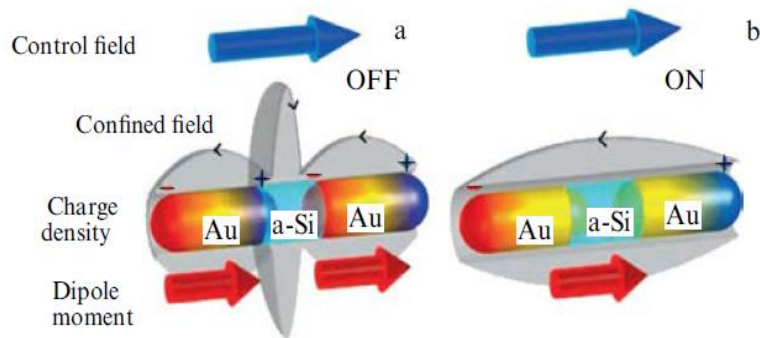
*Nonlinear Optical Metallic Dielectric Nano Dimer* (Noskov et al., 2012).



- **Non-linear optical response in semiconductor** - Semiconductors are the other type of materials which are used for non-linear feedback of the nanoantenna's. have semiconducting field maintains a movement of current by avoiding the dipole. For semiconducting system, the field strength depends on type of mode in the system.

**Figure 2.6**

Design Of A Nonlinear Optical Dipole (Large Et Al., 2010)



### 2.3 Nanoparticle Antennas in COMSOL

In this review, the author has used cross shaped aperture to enhance the strength of the electric fields and controlling the radiation pattern through excitation of LSPR's. the introduced emitter in the antenna couples with the system and determines the radiation pattern (Novotny & Van Hulst, 2011).

Localised surface Plasmon resonance (LSPR) is the coherent excitation of the surface electrons in the metallic nanoparticles. It enhances the metallic nanostructure scattering cross section by large proportions than the physical cross section (Bohren, n.d.). Any application which is depended on far field radiation pattern would benefit from this property like photo detection (Matsue, 2012), sensing (Matsue, 2012), vice versa. A model is built in COMSOL Multiphysics, using silver as its material for cross structure aperture particle having parameters like arm lengths, widths, and height positioned in vacuum is simulated. The finite element method (FEM) is used to simulate for scattering of cross section of the particle.

**Figure 2.7**

*Far Field Scattering Cross Section Of A Silver Cross As A Function Of Wavelength (Djalalian-Assl Et Al., 2011)*

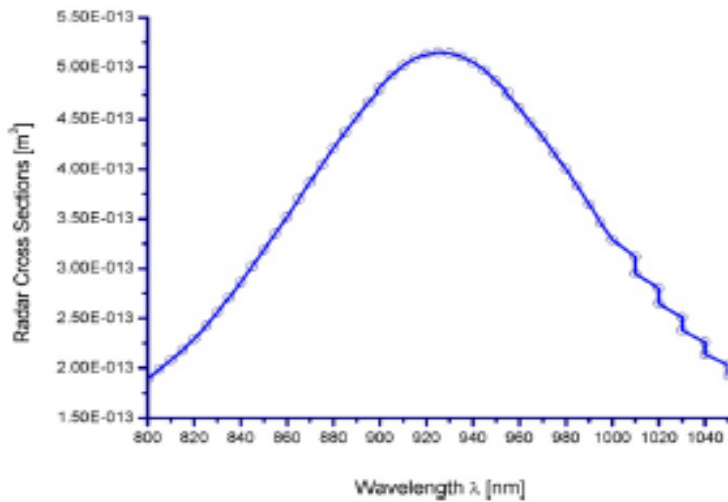
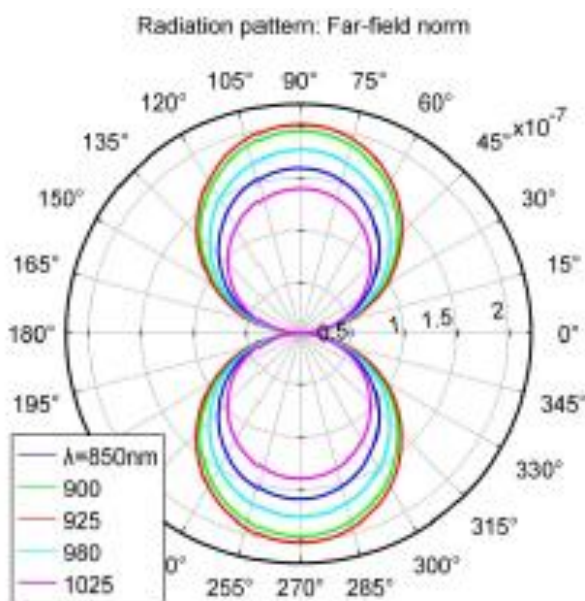


**Figure 2.8**

*The Scattering Far Field Radiation Pattern (Djalalian-Assl Et Al., 2011)*

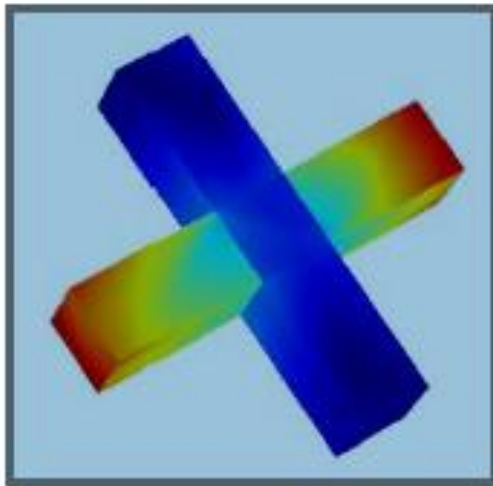


The incident field direction is taken as normal to the axes of the cross section of the aperture. The polarization is parallel to one of the arms and cross section can be regarded as consisting of two perpendicular Nanorods and independent of the polarization of the incident field. The far-field scattering pattern can be observed from

the figure 2.1 From the above images we can observe that the LSPR occurs at free space wavelength, 925 nm i.e. a blue shift of 155 nm when compared to cross shaped resonance having in the same directions. The far-field radiation pattern is shown in the above figure 2.8. The radiation pattern possesses a strong similarity to the electric dipole and figure 2.9. shows the electric field on the surface of the nanoparticle where the dipole excitation can be seen clearly.

**Figure 2.9**

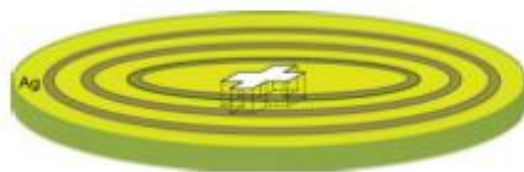
*The Electric Field At Resonance On The Surface Of Nanoparticle, Where Red Denoted Maximum Value (Djalalian-Assl Et Al., 2011)*



Finally, in this review, the author proposed a slot antenna which the benefits of radioactive decay rate with beam shaping(Lezec et al., 2002), comprising of one or both sides of the metal film. In the fig.2.9, we can see the illustration of the slot antenna.

**Figure 2.10**

*Slot Antenna With Surface Corrugations To Control Radiation (Djalalian-Assl Et Al., 2011)*

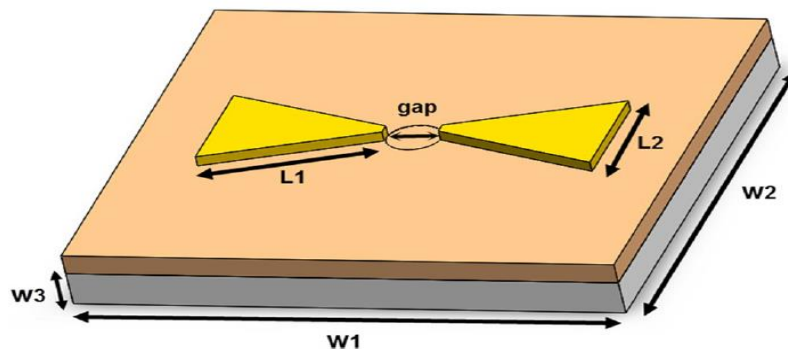


## 2.4 Tuneable Nano Antenna

In this paper, we study bow tie nanoantenna and how it controls the radiation pattern. In this author has investigated that by changing the nanoparticles in the nanoantenna has no effect in the direction of radiation pattern. The direction of the radiation pattern can be controlled by adding a nanoparticle in specified angle and with the help of piezoelectric layer which provides a gap between the nanoparticles. In this model, rotation of newly added nanoparticle near the origin causes the radiation pattern change to any required angles(Beheshti Asl et al., 2019).

**Figure 2.11**

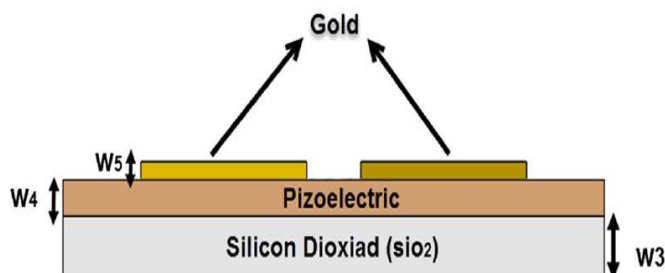
*Nano Antenna Structure (Beheshti Asl Et Al., 2019)*



In here,  $L_1$ ,  $L_2$ ,  $W_1$ ,  $W_2$ ,  $W_3$  are the parameters of the nanoantenna. The nanoparticles which acts as Nano antennas are of Gold particles. The radiation pattern in this structure is not controllable. For this, author have developed a novel structure which can be observed in the fig 2.6.

**Figure 2.12**

*Piezoelectric Layer Between Gold Bowtie Nano Antenna And Silicon Dioxide Substrate For Tuning (Beheshti Asl Et Al., 2019)*



Piezoelectric layer is deposited between the gold Nano antennas and silicon dioxide layers to control the antennas radiation pattern.

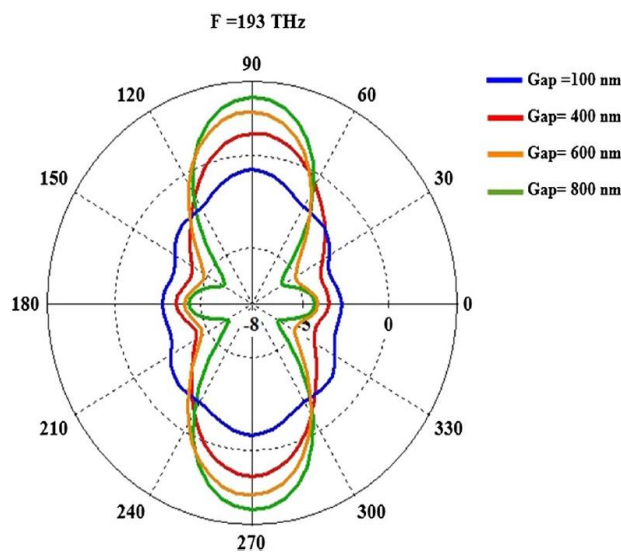
Finite integration technique (FIT) is used for this model to be simulated in CST studio to analyse in microwave module in the frequency of optics. FIT is very similar to FDTD method. FIT converts Maxwell's equation into much simpler form and analyse.

#### 2.4.1 Boundary Conditions

To prevent the reflected waves, enter the simulation region, PML layer is used in the model design. Far field domain boundary condition is used to get the results of the antenna as a radiation pattern.

**Figure 2.13**

*The Far Field Pattern For Nano Antenna With A Gap Between 100 And 800 Nm At 193 Thz (Beheshti Asl Et Al., 2019)*



#### 2.4.2 The Novel Design of Nano Antenna

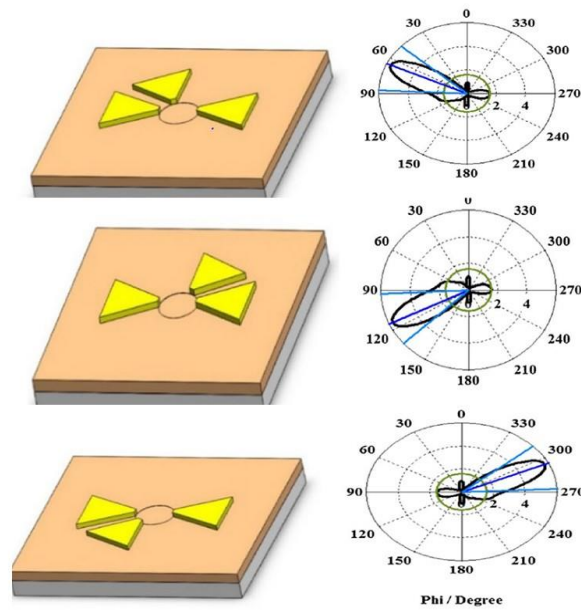
In this paper, a third nanoparticle with 60 degrees angle is added to control the radiation pattern of gold bow tie antenna. the piezoelectric layer is completely utilized, in order to have better analysis of the gap changes. “The piezoelectric effect is the ability of the certain materials to generate an electric charge in response to applied mechanical stress and tension”. Piezoelectric effect is used to change gap between the nanoparticles and



the direction of the pattern is controlled by the distance between nanoparticles (Beheshti Asl et al., 2019).

**Figure 2.14**

*Effect Of Changing The Geometric Of Added Nanoparticle On The Pattern Of The Nano-Antenna Simulated At 193 Thz (Beheshti Asl Et Al., 2019)*



From the above fig.2.14, we can observe that by changing the direction of the added nanoparticle, the direction of radiation pattern changes and we can obtain desired angles.

## 2.5 Modelling of Nanoantenna Arrays in COMSOL Multiphysics

In this paper, Nanoantenna arrays are modelled in COMSOL environment using Rf module and a related sensing system (Liu et al., 2009). A unit cell of Nano antenna is designed in the model builder. The incident light is a plane wave propagating along the Z direction. 3-D harmonic propagation mode is used in Rf module to simulate. There are two types of boundary conditions either can be used they are perfect electric conductor (PEC) and perfect electric magnetic conductor (PMC). wave is excited from the top surface and PML layer is used to prevent the reflected waves to enter in simulated region(Liu et al., 2008).

**Figure 2.15**

*Unit Cell Of Nanoantenna Array (Liu Et Al., 2009)*

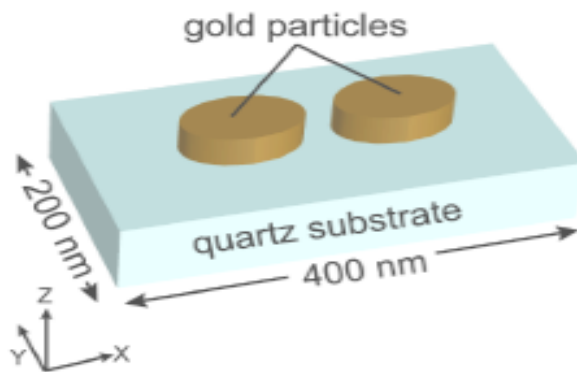
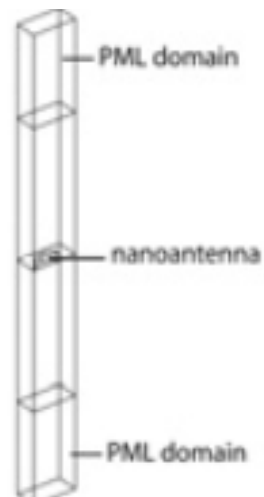


**Figure 2.16**

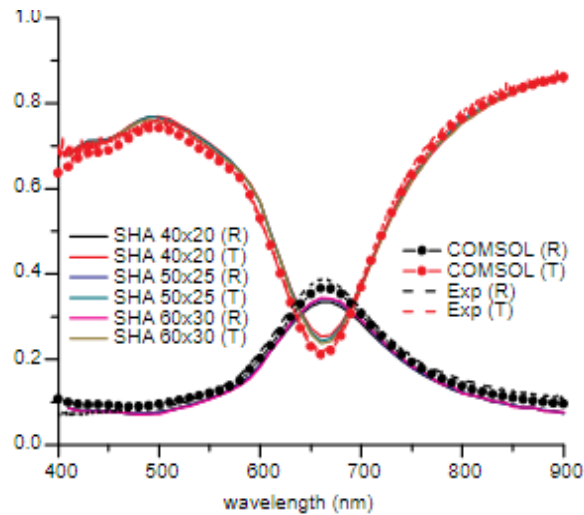
*The Structure Of Nanoantenna In COMSOL (Liu Et Al., 2009).*



The reflectance and transmittance are extracted from the results, and they are compared to experimental spectrum obtained with spatial harmonic analysis (SHA) (Liu et al., 2009), which also known as rigorous coupled wave analysis (RCWA) (Nojonen & Turunen, 1994).

**Figure 2.17**

*The Reflectance And Transmittance Spectra Extracted From COMSOL, And SHA (Liu Et Al., 2009)*



The comparison of results from COMSOL and SHA experimental is shown in Fig.2.17 which is proof of simulation authenticity provided by the COMSOL.

## 2.6 Photoconductive Antenna (PCA) Using Optical Antenna Array of ZnO Nanorods

In this work, ZnO nano rods array has been used on a PCA as an optical antenna which helps to enable the proficiency of the local field and femtosecond laser is used in LT-GaAs layer. the optical power and hands meant results in higher power for Terahertz emission for more photo carrier generation (Bashirpour et al., 2019).

**Figure 2.18**

*Schematic Proposed PCA In 3-D View (Bashirpour Et Al., 2019)*

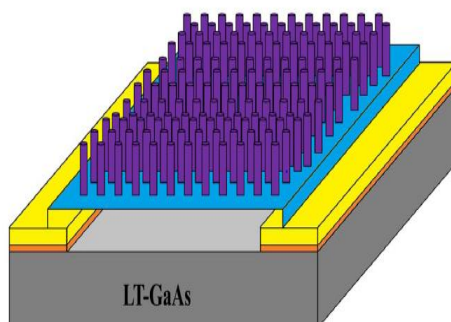
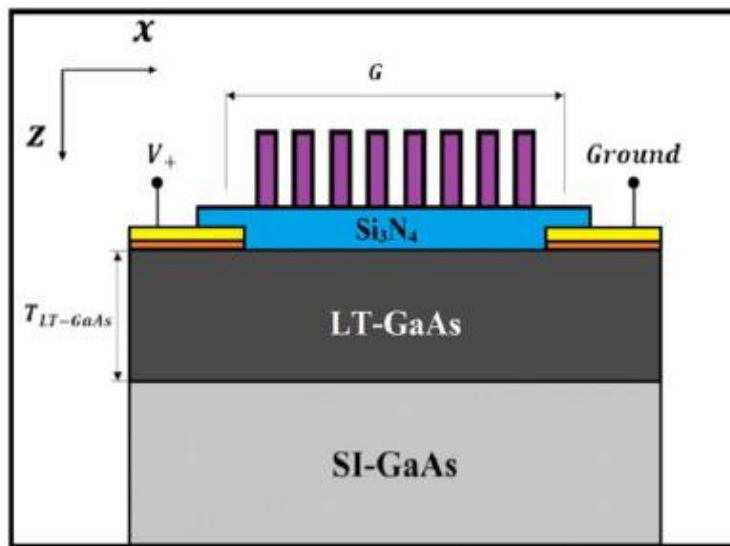


**Figure 2.19**

*Schematic Diagram Of PCA In Front View (Bashirpour Et Al., 2019)*



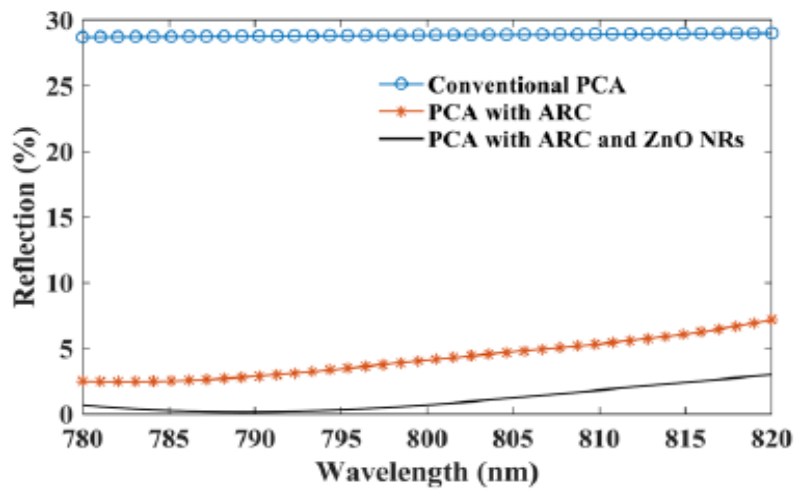
### **2.6.1 Device Structure and Design**

Propose the structure of device shown in figure 2.12, LT-GaAs layer is used and deposited on semi insulating GaAs substrate. in this design, Titanium layer is used as gold adhesion. Few parameters like thickness, length, and width of dipole antenna are taken. A Silicon nitride layer is considered as ARC and is used to minimize the reflection from surface. Silicon nitride layer isolate the gap between ZnO nano rods. Finally, ZnO nanorods were grown on silicon nitride layer.

Finite element analysis (FEM) was used to study the electrical and optical behaviour of the design by using Maxwell's equation and poission equation. when compared to PCA with and without ARC, the design observes a 2.5-fold and 6-fold increase.

**Figure 2.20**

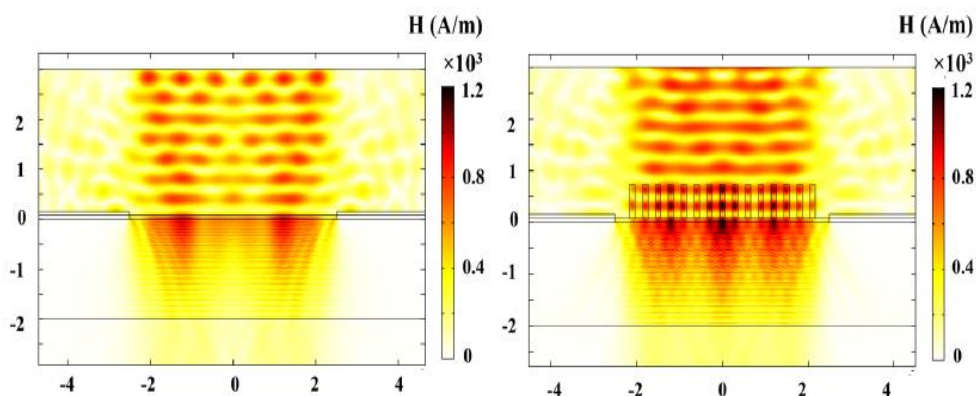
*Reflections Of PCA With And Without ARC (Bashirpour Et Al., 2019)*



From the above fig.2.14, we can observe that reflection is less than 0.8% compared to the 4% of PCA with silicon nitride ARC layer and 29% of the regular PCA without ARC.

**Figure 2.21**

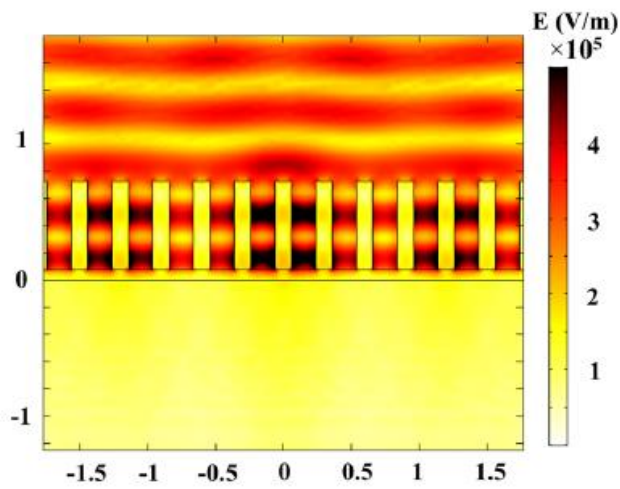
*Simulated Magnetic Field Distribution Of Regular PCA Without And With ZnO NrS (Bashirpour Et Al., 2019)*



From fig 2.22, the nano rods array behaves as dielectric nano antenna and by concentrating laser pulse it can create strong near field enhancement. Red colour shows the maximum intensity of the magnetic field.

**Figure 2.22**

*The Electric Field Distribution Of ZnO Nanorods (Bashirpour Et Al., 2019)*



Form the above fig.2.22, We can observe the electric field distribution of ZnO NRs in the simulated results. Red colour shows the maximum intensity of the electric field.

In summary, to enhance the performance of PCA a unique idea of optical nano antennas in the form of dielectric nanorods is presented. effect of ZnO nanorods on the PCA with and without ARC is studied through simulation method. From the simulation results we can observe the decrease in the reflection of ZnO NRs with ARC is very less compared to PCA with ARC.

## CHAPTER 3

### METHODOLOGY

The methodology for this research work can be divided into three stages, as shown below,

- Material selection
- Construction and modelling of optical nanoantenna
- Construction and modelling of an array of nanoantenna

#### 3.1 Material Selection

In this study, we constructed the nanoantenna using semiconductor materials. Silicon (Si) is a widely used semiconductor material in the field of electronics and optoelectronics because of its superior electronics properties. However, Si has a strong absorption in the visible to NIR region which makes it inappropriate for optical nanoantenna applications. Other two commonly used oxide-based semiconductors are titanium dioxide (TiO<sub>2</sub>) and zinc oxide (ZnO).

Both these two materials show some similar properties, but TiO<sub>2</sub> has a lower electron mobility than ZnO. Besides ZnO is a material with wide band gap of 3.37 eV at room temperature. It has a large excitonic binding energy of 60 meV which is greater than thermal energy at room temperature. A single crystal of ZnO exhibit significantly faster electron transport and greater mobility (~200 cm<sup>2</sup>/V/s). The faster the electrons transport the higher the mobility, which results in high electron diffusion coefficients which can provide significant advantages to device performance.

The greater electron mobility is due to the direction uninterrupted conduction channel, which can improve the efficiency of charge collection and enables the production of optically thick cells which absorb more incident light. Since ZnO could emits at the near ultraviolet, has transparent conductivity and piezo electric properties and has diverse material properties, thus, ZnO is an interesting material for semiconductor devices. In addition to that, it is also relatively easy to synthesize anisotropic nanorods of ZnO using simple wet chemical techniques, which later allows easy fabrication of ZnO nanorod-based optical nanoantenna's. We therefore selected ZnO as our material for further studies.

### 3.2 Construction of Optical Nanoantenna

After selection of the material, we constructed the nano-antenna elements using COMSOL environment. The construction of a nano-antenna element can be divided into four steps:

1. Model setup: creating the model with required geometry values, defining each material and their properties, adding the required physics and study, defining the equations to solve, setting up a required boundary and port conditions.
2. Meshing: using finite elements, the clustering of the model space is done in meshing.
3. Solving: a set of linear equations is solved by a default solver using the study which we have taken earlier which describes the electric field norm.
4. Post-processing: useful information is obtained from the computed electric fields.

#### 3.2.1 Model Setup

Building the model in 2-D axis symmetry using COMSOL Multiphysics. We built a rectangular rod and considered it as nanorod with length = 600nm and width = 60nm. We defined the material as ZnO. Another circle surrounding the nanorod with a radius = 1200nm was constructed and we defined the material as air.

**Table 3.1**

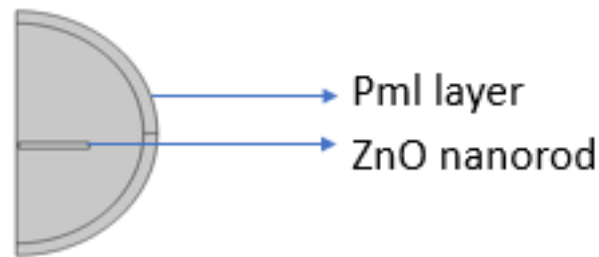
*Material Properties of ZnO Nanoantenna in COMSOL*

<b>Materials</b>	<b>Refractive index (real part)</b>	<b>Refractive index (imaginary part)</b>
<b>ZnO</b>	1.95	0
<b>Air</b>	1	0



**Figure 3.1**

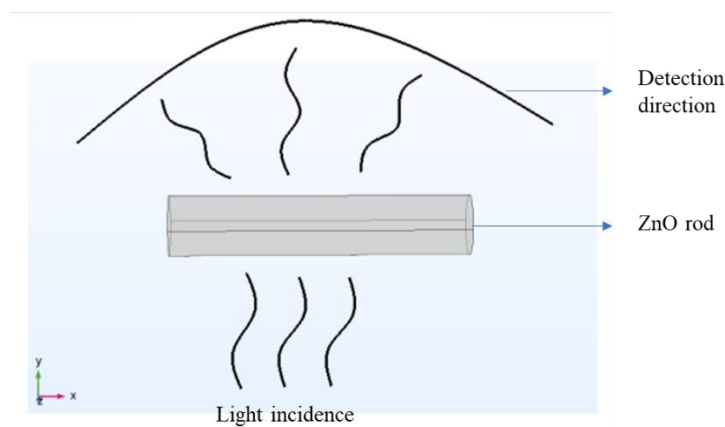
*Geometry of The Model Designed in COMSOL Multiphysics*



We then used Electromagnetic waves and frequency domain module for simulation. In the electromagnetic waves, we encounter two types of case studies, RF or wave optics modules and ray optics module. In our case, we used a wave optics module, for solving Maxwell's equation.

**Figure 3.2**

*Simulation Mechanism of Single ZnO Rod*



It is always very necessary to provide boundary conditions to the model as to obtain the desired results. We define scattering boundary condition around the exterior part that domain which will be used to make the boundary transparent for a scattered wave. The boundary condition is also transparent for an incoming plane wave. We used far field domain to extract radiation patterns in 2-D and 3-D axis.

### 3.2.2 *Meshing*

When solving electromagnetic wave problems, mesh resolution is very important. Fine mesh is required for any model in the simulation and for wave models a good mesh is used to solve the wavelengths in the model. Mesh size depends on the wavelength used; it should be at least half of the wavelength measurement.

2nd order element is used by COMSOL Multiphysics to separate the equations which we are using for solving. A coarse mesh was used to equate the equation, but this would result in low accuracy. To resolve for a propagating wave in a dielectric medium, at least five 2nd order mesh sizes were used. 1st order and 3rd order discretisation were also available but mostly 2nd order element is finest understandably between precision and required memory.

In our model, we preferred tetrahedral mesh rather than the hexahedral mesh due to their lower dispersion error. For tetrahedral mesh, the maximum distance is same in all the directions within an element.

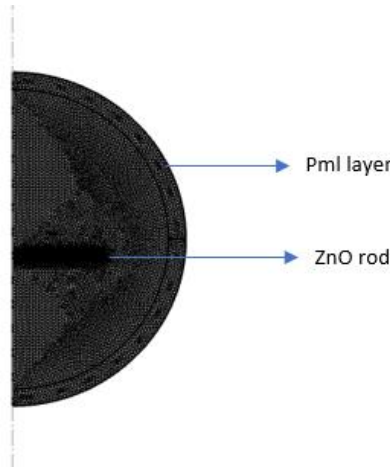
In meshing requirements, there are two types:

- Physics controlled mesh
- User-controlled mesh or manual mesh

Physics controlled mesh is the mesh that is controlled by software and it will be constructed according to the study which we take. The manual mesh is the mesh that is constructed by the user according to the study and the results which the user wants.

**Figure 3.3**

Meshed Geometry of The Model.



### 3.2.3 Solving

A finite element analysis approach was used to solve the model in electromagnetic waves and frequency domain

$$\omega = 2\pi f \quad (1)$$

Where,  $\omega$  = Angular frequency;

$f$  = Frequency of the wave;

The Maxwell's equation in the domain is reduce to

$$\nabla \times (\mu_r^{-1} \nabla \times E) - \frac{\omega^2}{c_0^2} (\epsilon_r - \frac{i\sigma}{\omega\epsilon_0}) E = 0 \quad (2)$$

Where,  $\mu_r$  = relative permeability;

$\epsilon_r$  = relative permittivity;

$\sigma$  = electrical conductivity; and

$C_0$  = speed of light in vacuum;

Throughout the modelling domain, Electric field,  $E = E(x, y, z)$ , is computed from equation (2), where  $E$  is a vector with components  $E_x$ ,  $E_y$ , and  $E_z$ . Electric field derives different quantities like magnetic fields current and power flow of the domain. It is additionally conceivable to reframe the equation (2) as an eigenvalue and it is solved for different wavelengths.

Wave equation for the above-constructed model for the electric field is

$$\nabla \times (\nabla \times E) - k_0^2 \epsilon_r E = 0 \quad (3)$$

$$\epsilon_r = (n - ik)^2 \quad (4)$$

Where, n= refractive index of the real part

k= refractive index of the imaginary part

The wave equation varies with the refractive index of the model. the refractive index of Air is n=1 and k=0 as mentioned in Table 1.

The refractive index for ZnO varies from different values for a different set of wavelengths. For this, COMSOL Multiphysics uses interpolation function for the refractive index of ZnO and defines a set of values for different wavelengths.

PML layers are considered to truncate the domain and avoid internal reflections.

Mie theory of scattering is a solution of maxwells equation applied to the scattering of plane waves. It can be applied to any value of the particle diameter relative to the scattered light wavelength and valid to any particle refractive index.

Mie solution to maxwells equations provides the basis for measuring the scattering of electromagnetic radiation.(Ichimaru, 2019)

In scattering problems, the total wave decomposes onto incident and scattered waves

$$E = E_{inc} + E_{sca} \quad (5)$$

$$H = H_{inc} + H_{sca} \quad (6)$$

Maxwells wave equation is solved with respect to scattered electric field

$$\nabla \times (\mu_r^{-1} \nabla \times E_{sca}) - \frac{\omega^2}{c_0^2} (\epsilon_r - \frac{i\sigma}{\omega\epsilon_0}) E_{sca} = 0 \quad (7)$$

The scattered magnetic field is calculated from Faradays law

$$H_{sca} = -\frac{1}{j\omega\mu} \nabla * E_{sca} \quad (8)$$

The time average pointing vector for time harmonic fields gives the energy flux

$$p = \frac{1}{2} \text{Re}[E * H], [\text{W}/\text{m}^2] \quad (9)$$

$$H_{inc} = \frac{1}{\eta} K * E_{inc} \quad (10)$$

Where,  $K$  is the direction of incident wave propagation,

$\eta = \sqrt{\mu/\epsilon}$  is characteristic impedance,

$$p_{inc} = \frac{1}{2\eta} (|E_{inc}| * |E_{inc}|)K \quad (11)$$

### 3.2.4 Cross Section Calculations

Physical quantities can be obtained from scattered fields, cross section, which can be defined as the net rate at which electromagnetic energy ( $W$ ) crosses the surface of an imaginary sphere centered at the particle divided by the incident irradiation ( $p_{inc}$ ). To quantify the rate of the electromagnetic energy that is absorbed ( $W_{abs}$ ) and scattered ( $W_{sca}$ ) by the particle, the absorption ( $\sigma_{abs}$ ) and scattering ( $\sigma_{sca}$ ) cross section can be defined (Ichimaru, 2019)

$$\sigma_{sca} = \frac{W_{sca}}{p_{inc}} \quad (12)$$

$$\sigma_{abs} = \frac{W_{abs}}{p_{inc}} \quad (13)$$

Where,  $p_{inc}$  is the incident irradiance defined as energy flux of the incident wave,

$W_{abs}$  is energy rate absorbed by the particle

$W_{sca}$  is the scattered energy rate.

The total scattering cross section, or excitation cross section, is the amount of energy removed from the incident field due to absorption and scattering.

$$\sigma_{ext} = \sigma_{abs} + \sigma_{sca} \quad (14)$$

The total absorbed energy derived by integration of energy loss over the volume of the particle.

$$W_{abs} = \iiint_{V_p} Q_{loss} dV \quad (15)$$

$$Q_{loss} = \frac{1}{2} Re [J_{tot} \cdot E + j\omega B \cdot H] \quad (16)$$

$$W_{abs} = \frac{1}{2} \iiint_{V_p} Re [J_{tot} \cdot E + j\omega B \cdot H] dV \quad (17)$$

The scattered energy is derived by integration of the pointing vector over an imaginary sphere around the particle

$$W_{sca} = \oiint p_{sca} \cdot \mathbf{n} dS \quad (18)$$

$$W_{sca} = \frac{1}{2} Re [E_{sca} * H_{sca}] \cdot \mathbf{n} dS \quad (19)$$

Where  $\mathbf{n}$  is unit vector normal to the imaginary sphere.

### 3.2.5 Far Field Radiation Calculations

COMSOL includes a built-in far field computation function that automatically calculates the far field variables defined as

$$E_{far} = \lim_{r \rightarrow \infty} r E_{sca} \quad (20)$$

The far field variables,  $E_{far}$  represent the scattering amplitude.(Comsol, 2013)

By using the above equations, we simulated the model and extracted the scattering cross section of the rectangular rod (Asapu et al., 2016).

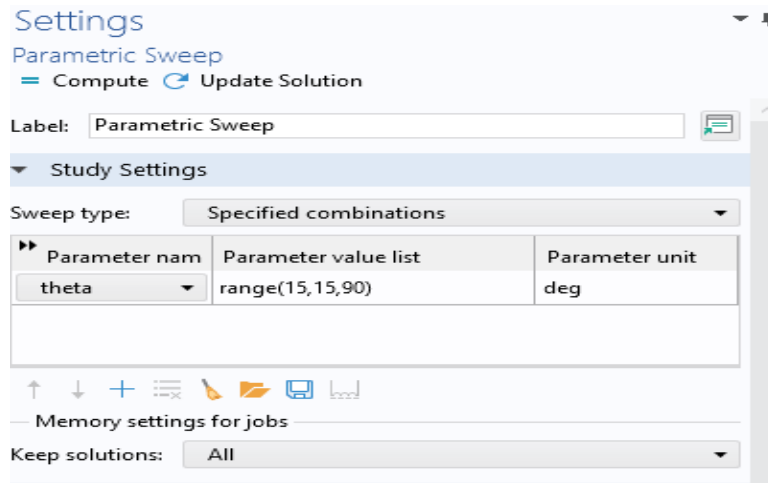
### 3.2.6 Post Processing

After solving the model, the data needs to be extracted from the electromagnetic fields. The software automatically produces the multislice plot of the electric field. With the help of a multislice plot, we can change our plane and see the results in all directions and given wavelengths.

We added parametric sweep in the study to simulate for angel of incidence (Theta). We defined theta parameter in the parameters section, by taking that parameter different angle of incidence results can be obtained.

**Figure 3.4**

*Parametric Sweep in Settings*

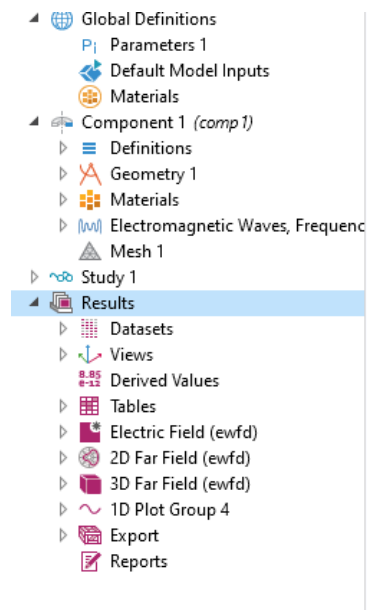


We can also extract different plots in the results as shown in the Figure 3.3. We can select a 1D plot group and select global to extract the given properties like scattering, absorption and extinction of the cross section of the rod.

We can extract far field patterns for spherical model, far field domain produces 2D radiation pattern and 3D radiation pattern. We can export all the required data into system.

**Figure 3.5**

*Postprocessing View of The Model*



### 3.3 Construction of Array of Nanoantenna

For constructing and modelling of an array of nanoantenna in COMSOL Multiphysics, after mentioning the geometry of a single antenna there is a function in geometry called array. We selected the array function and created 1\*5 array and simulated.

**Figure 3.6**

*Geometry of Nanoantenna Array*

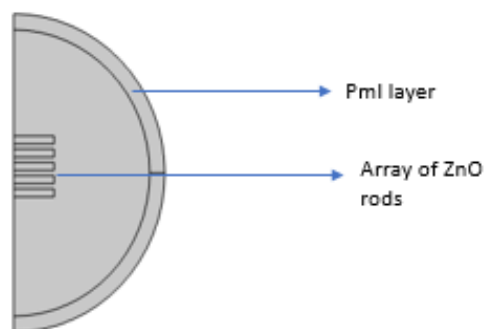
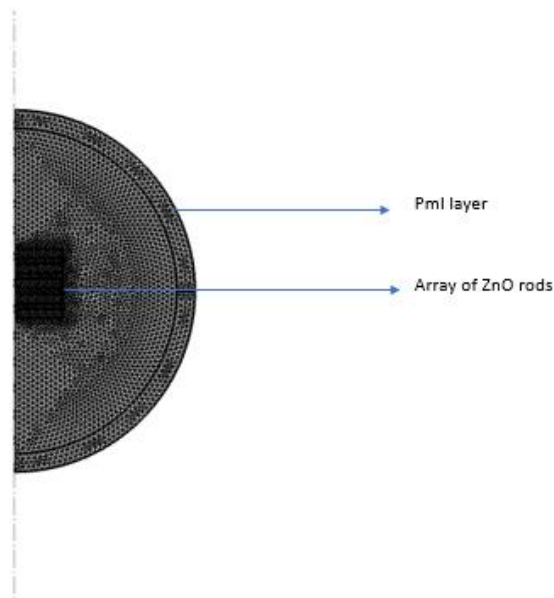




**Figure 3.7**

*Meshed Geometry of Nanoantenna Array*



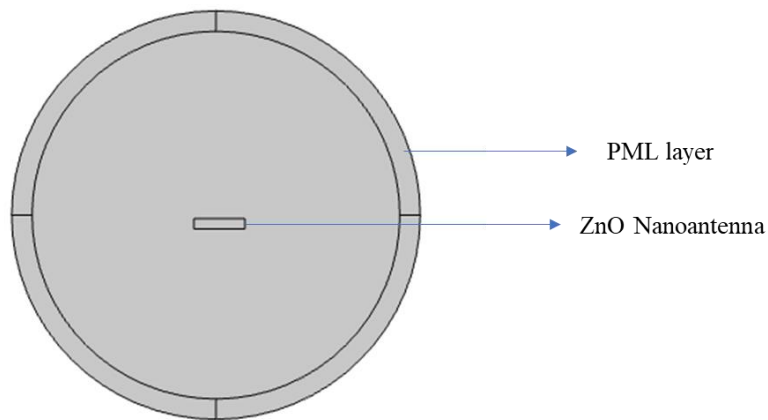
After constructing the required array of nanoantenna, all the above steps which are mentioned earlier are repeated to obtain the simulation results.

We investigated the effects of size, spacing, orientation of the rod and shape of the rods for its radiation patterns. The simulation mechanism for all the effects will be same i.e. the light incidence and detection region are fixed. Only nanoantenna elements are varied from size orientation space between array.

We simulated for different lengths of the rod i.e. 300nm, 600nm, and 1200nm after construction of model we simulated and extracted the results.

**Figure 3.8**

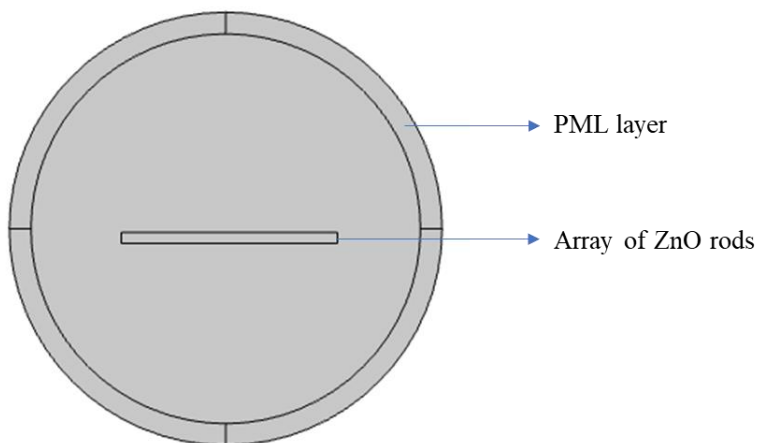
*Geometry of Single Nanoantenna With Length 300nm*



From Figure 3.8, the construction of single nanoantenna rod in 2-D with varying length of the rod from 600nm to 300nm.

**Figure 3.9**

*Geometry of Single Nanoantenna with Length 1200nm*

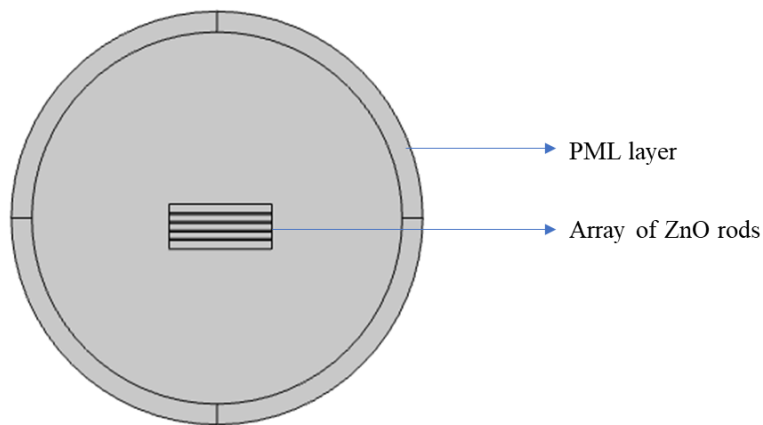


From Figure 3.9, the construction of single nanoantenna rod in 2-D with varying length of the rod from 600nm to 1200nm.

We investigated by varying the space between the nanoantennas of the array from 50nm, 100nm and 200nm.

**Figure 3.10**

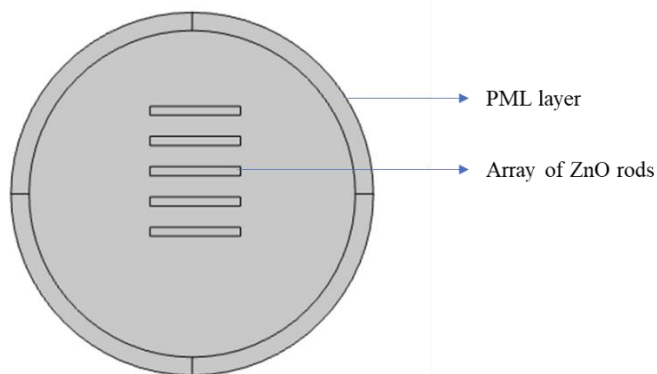
*Geometry of 1\*5 array of Nanoantenna Element with Spacing of 50 nm*



From Figure 3.10, the construction 1\*5 array of nanoantenna rods are in 2-D with the spacing between the rods are changed to 50nm from 100nm.

**Figure 3.11**

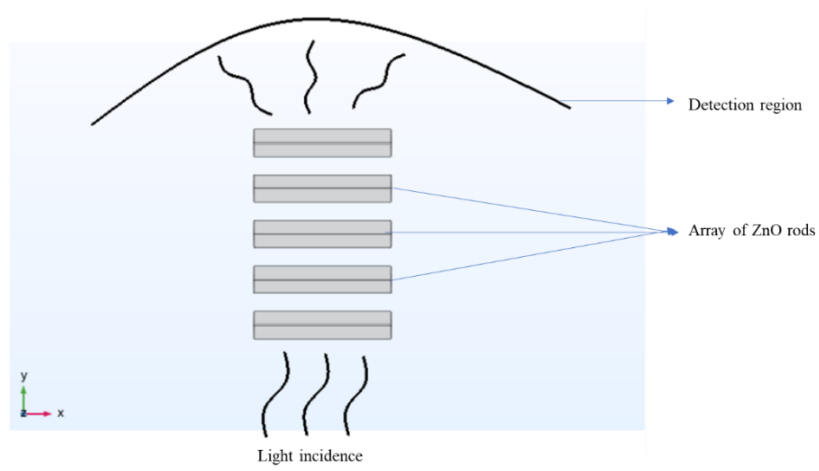
*Geometry Of 1\*5 Array of Nanoantenna Element with Spacing Of 200 nm*



From Figure 3.11, the construction 1\*5 array of nanoantenna rods are in 2-D with the spacing between the rods are changed to 200nm from 100nm. We investigated by varying the angle of incidence ( $\Theta$ ) of wave propagation, by using parametric study where we vary theta from  $15^\circ$  -  $90^\circ$  for 1\*5 array of nanoantenna with a spacing of 100nm. We simulated and extracted the required results.

**Figure 3.12**

*Simulation Mechanism of Array of ZnO Nanorods*



## CHAPTER 4

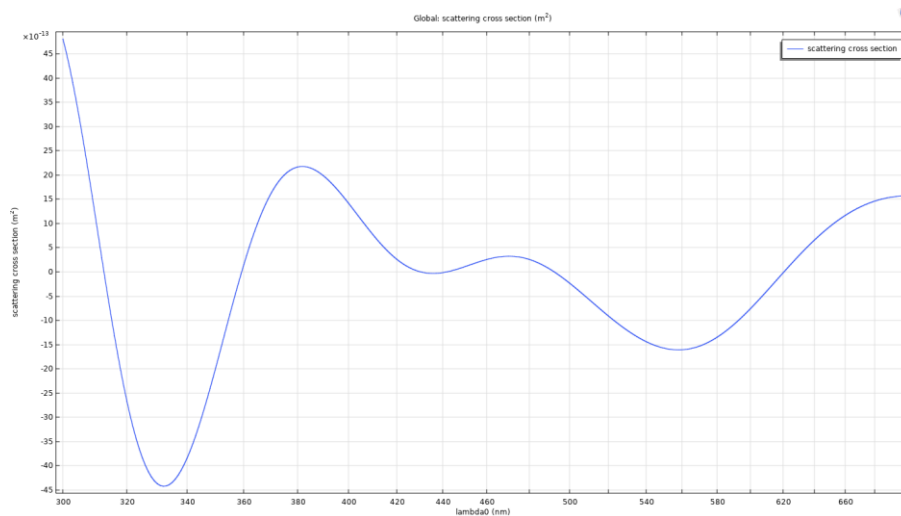
### RESULTS AND DISCUSSION

#### 4.1 Simulation Results of Single ZnO Nanorod Scattering and Radiation Patterns

Simulation and modelling of the single ZnO nanorod scattering is conducted in the simulation environment by using simulation tool. The evaluation of scattering cross section of ZnO nanorod in air with radius 60 nm and length 600 nm. Light is axially incident perpendicular to the rod axis. The material data is taken from the reference paper. Apart from the scattering and absorption of the rod we had extracted radiation pattern of the nanorod for wavelengths ranging from 300nm – 700nm. Fig 4.1 shows the scattering and radiation patterns of single ZnO nanorod.

**Figure 4.1**

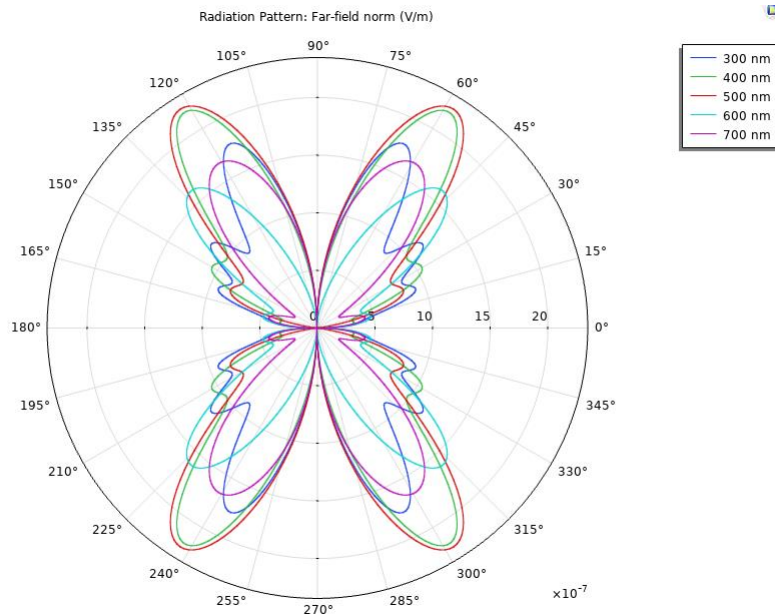
*Scattering Cross Section of The Single Nanoantenna Element*



We can observe the characteristic resonance of the nanoantenna in 2-D axis is at 380 nm. We can observe the peak at that wavelength.

**Figure 4.2**

*Far Field Radiation Pattern of Single Nanoantenna Rod at Wavelength 300nm – 700nm*



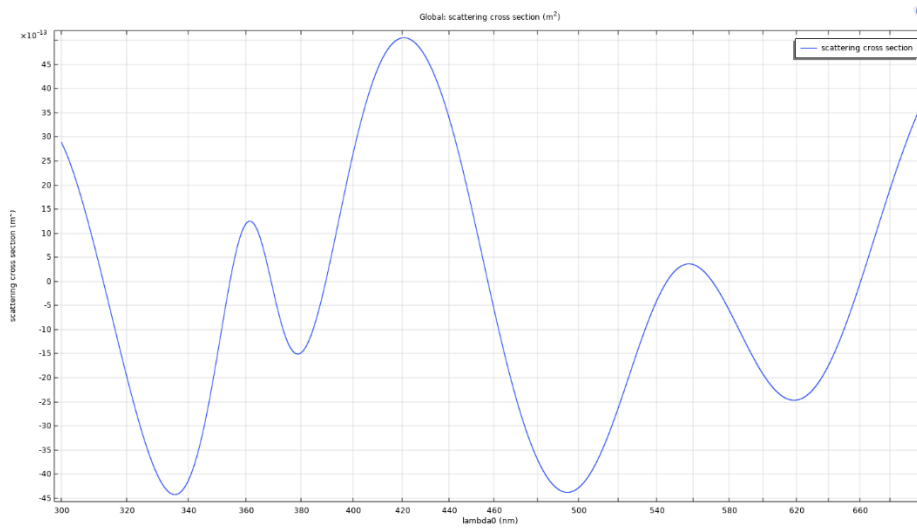
We can observe the radiation pattern of the single nanoantenna element from 300nm – 700nm wavelengths. We can observe the scattering amplitude of  $10^{-7}$  V/m.

#### **4.2 Simulation and Modelling Results of Nanorod Array Scattering and Radiation Patterns**

We extended the single nanoantenna element into an array of nanoantenna elements with spacing between the elements is 100nm. We constructed 1\*5 nanoantenna array and extracted scattering cross section and radiation pattern from 300nm – 700nm wavelengths which can be observe in figure 4.3 and figure 4.4.

**Figure 4.3**

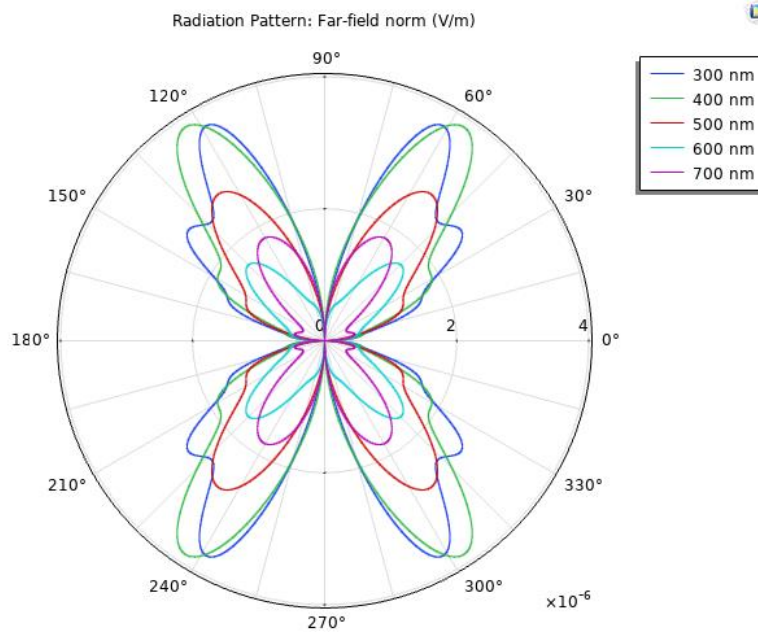
*Scattering Cross Section f 1\*5 Array of Nanoantenna Element*



We can observe that the characteristic resonance of 1\*5 array of nanoantenna is at 420 nm.

**Figure 4.4**

*Far Field Radiation Patter Of 1\*5 Array of Nanoantenna Element At 300nm -700nm Wavelengths*



We can observe the radiation pattern of 1\*5 array of nanoantenna elements from 300nm -700nm wavelengths. We can observe the scattering amplitude of  $10^{-6}$  V/m which is higher than the single nanoantenna element.

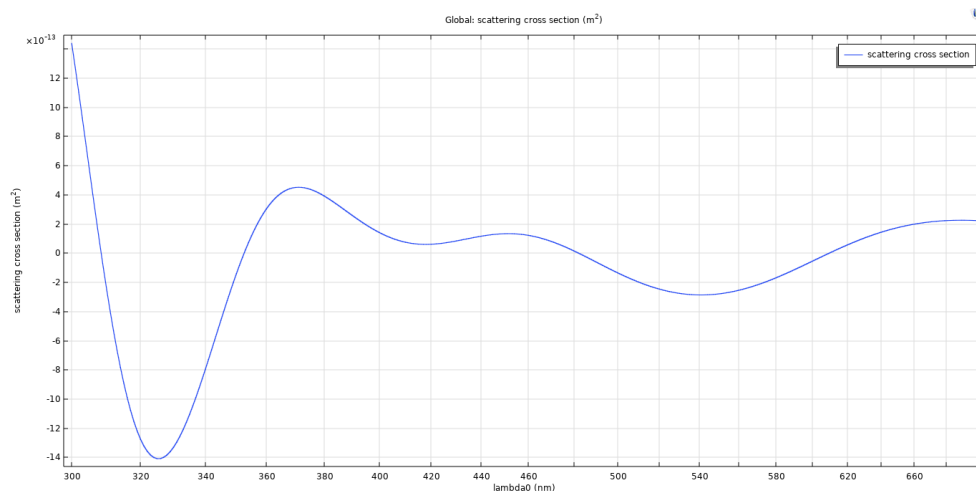
### 4.3 Simulation Results of the Effects of Size, Spacing between the Elements in Array, and Angle of Incidence of Wave Propagation of Array on Scattering and Radiation patterns

#### 4.3.1 Effect of Change in Size of the Single Nanoantenna element

After the simulations of single nanoantenna element and array of nanoantenna element, we simulated for the effect of the size, orientation of the rod and spacing between the rods in the array. we simulated by changing the single nanoantenna element size of the length from 600nm to 300nm and 1200nm and extracted the scattering and radiation patterns which can be observed in figures 4.5, 4.6,4.7 and 4.8.

**Figure 4.5**

*Scattering Crosssection Of Single Nanoantenna With Length 300nm*

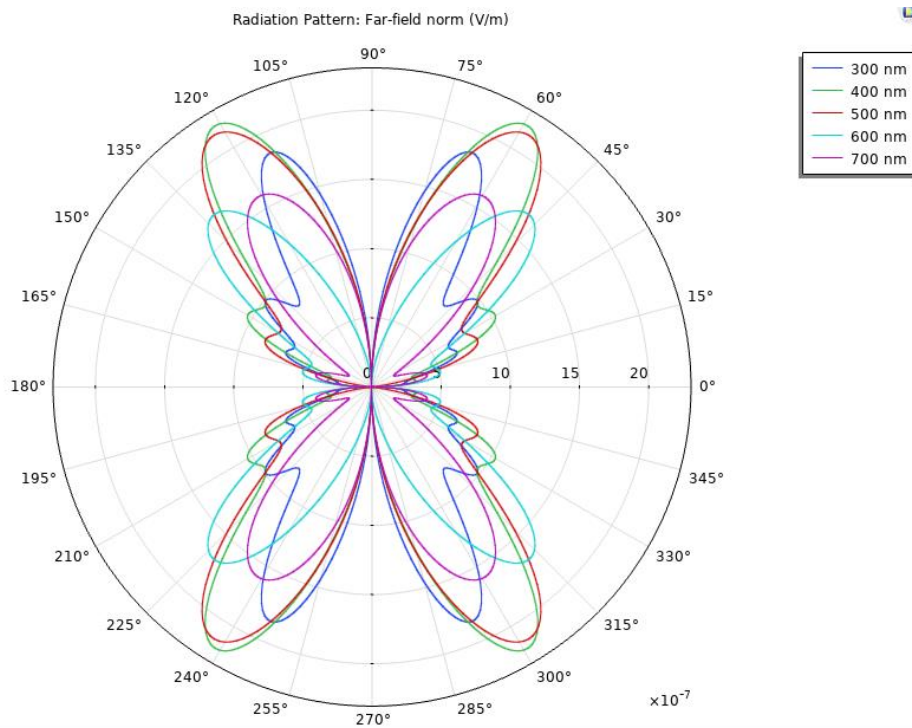


We can observe the characteristic resonance of the nanoantenna at 370 nm. We can observe the peak at that wavelength. When we compare this to 600nm length nanoantenna, the scattering peak moved to 370nm by reducing length of the rod to 300nm.



**Figure 4.6**

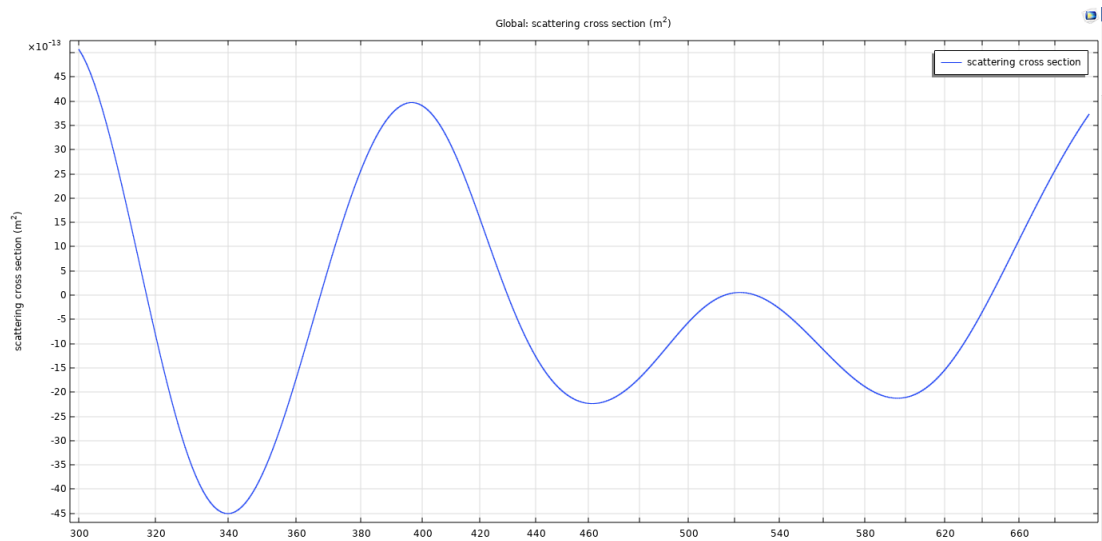
*Far Field Radiation Pattern for Single Nanoantenna Element with Length 300nm*



We Can Observe the Radiation Pattern of Single Nanoantenna Element with Length 300nm from 300nm -700nm Wavelengths. We Can Observe the Scattering Amplitude Of  $10^{-7}$  V/m.

**Figure 4.7**

*Scattering Crosssection Of Single Nanoantenna With Length 1200nm*

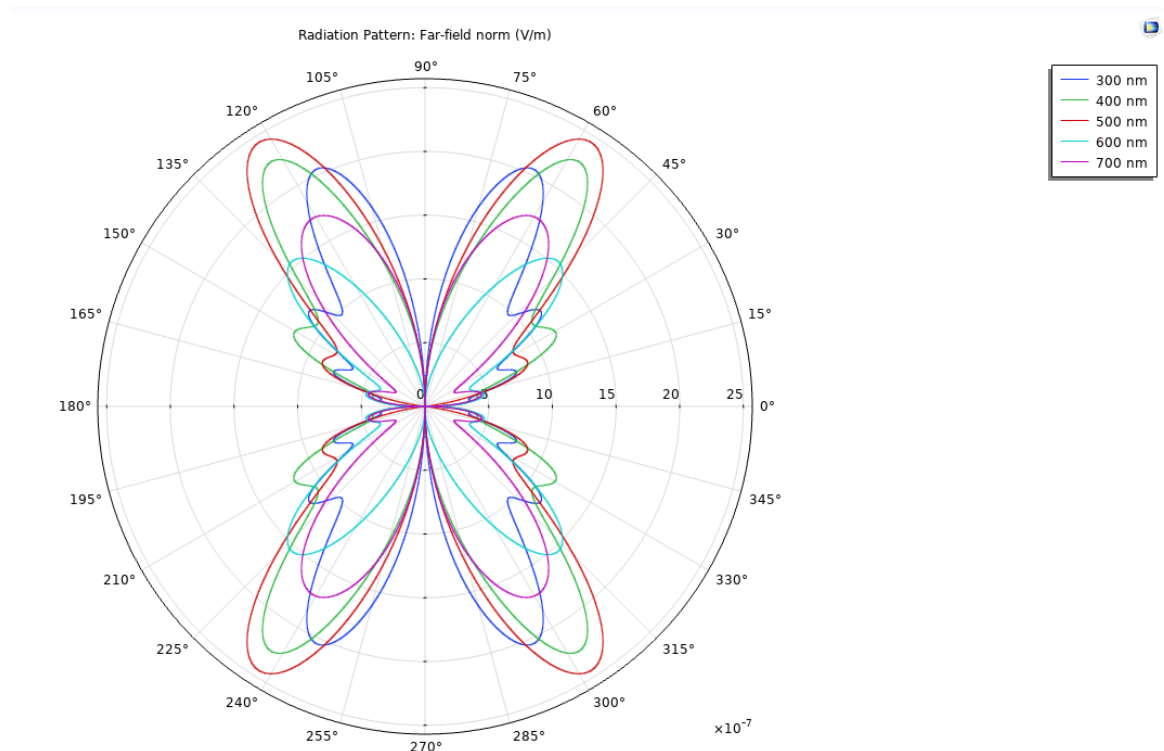


We can observe the characteristic resonance of the nanoantenna at 390 nm- 400 nm. We can observe the peak at that wavelength.

When we compare all the single nanoantenna with different sizes, depending on the size of the rod the scattering changes if we reduce the length of the rod, the scattering peak reduces and when length of the rod increases and scattering peak also increase.

**Figure 4.8**

*Far Field Radiation Pattern for Single Nanoantenna Element with Length 1200nm*



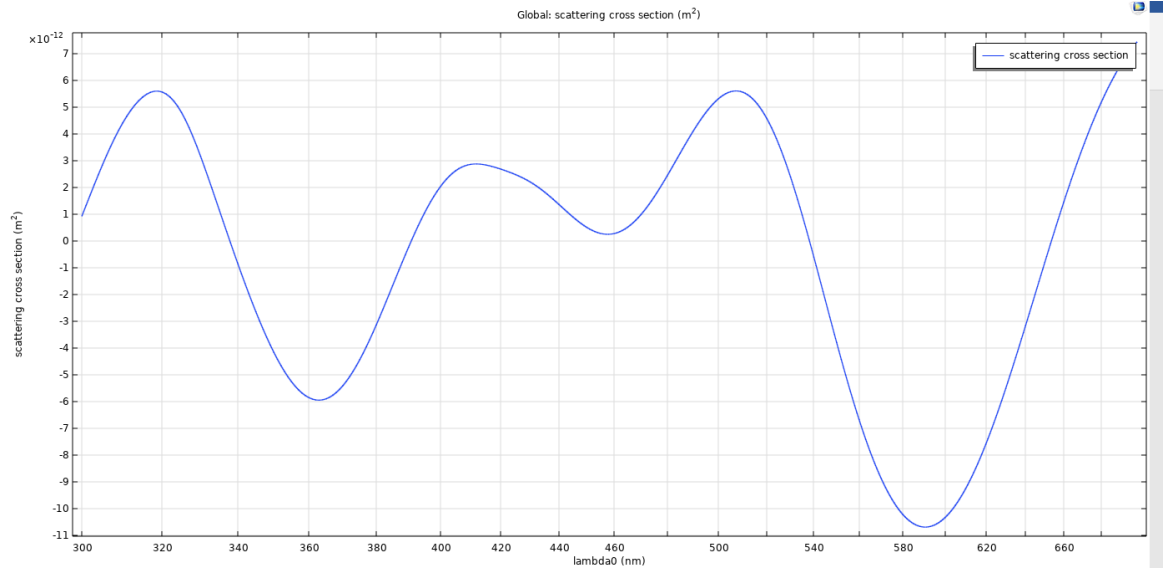
We Can Observe the Radiation Pattern of Single Nanoantenna Element with Length 300nm from 300nm -700nm Wavelengths. We Can Observe the Scattering Amplitude Of  $10^{-7}$  V/m.

#### ***4.3.2 Effect of Change in Spacing Between the Array of Nanoantenna Element on the Scattering and Radiation Pattern***

From the array of nanoantenna element, we change the spacing between the elements in that array and extracted scattering and radiation patterns which can be observe in figures 4.9,4.10, 4.11, 4.12.

**Figure 4.9**

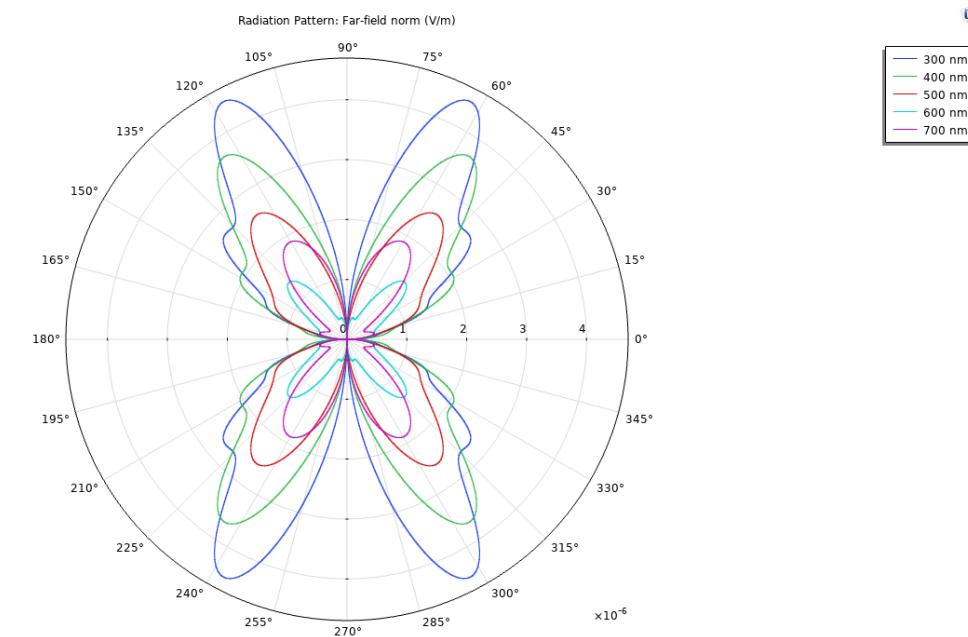
*Scattering Cross Section Of 1\*5 Array of Nanoantenna Element with Spacing Of 50 nm*



We can observe the characteristic resonance of the nanoantenna is at 320 nm and 500 nm. We can observe the peak at that wavelength.

**Figure 4.10**

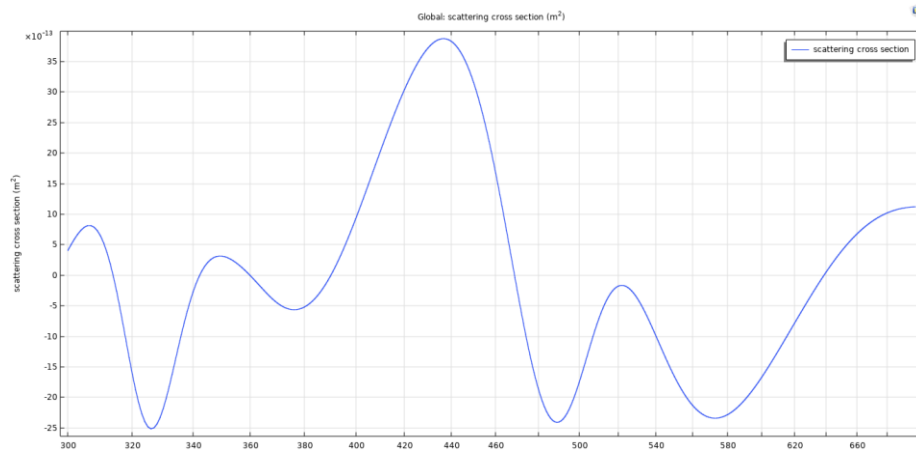
*Far Field Radiation Pattern Of 1\*5 Array of Nanoantenna Element with Spacing Of 50nm*



We Can Observe the Radiation Pattern Of 1\*5 Array of Nanoantenna Element with Spacing Of 50nm, From 300nm -700nm Wavelengths. We Can Observe the Scattering Amplitude Of  $10^{-6}$ V/m.

**Figure 4.11**

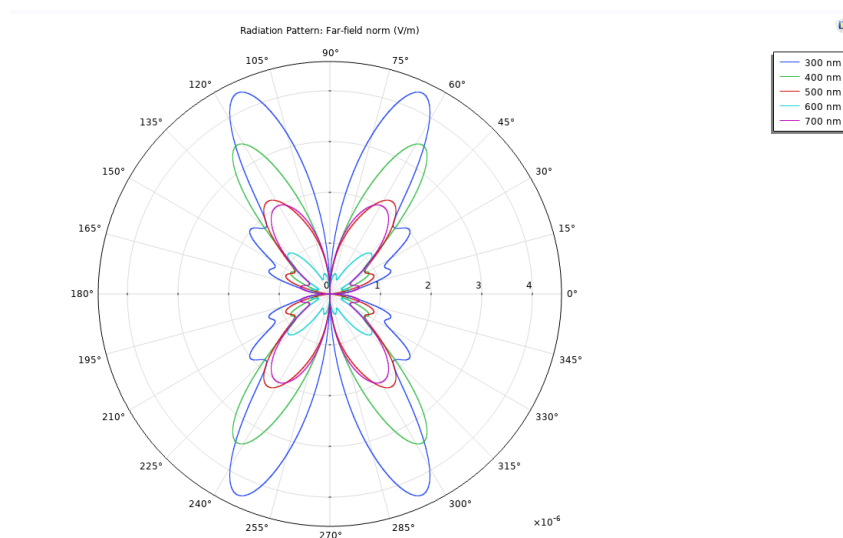
*Scattering Cross Section of 1\*5 Array of Nanoantenna Element with Spacing of 200 nm*



We can observe the characteristic resonance of the 1\*5 array of nanoantenna with spacing of 200nm between the elements at 430 nm - 440 nm. We can observe the maximum peak at that wavelength.

**Figure 4.12**

*Far Field Radiation Pattern of 1\*5 Array of Nanoantenna Element with Spacing of 200nm*



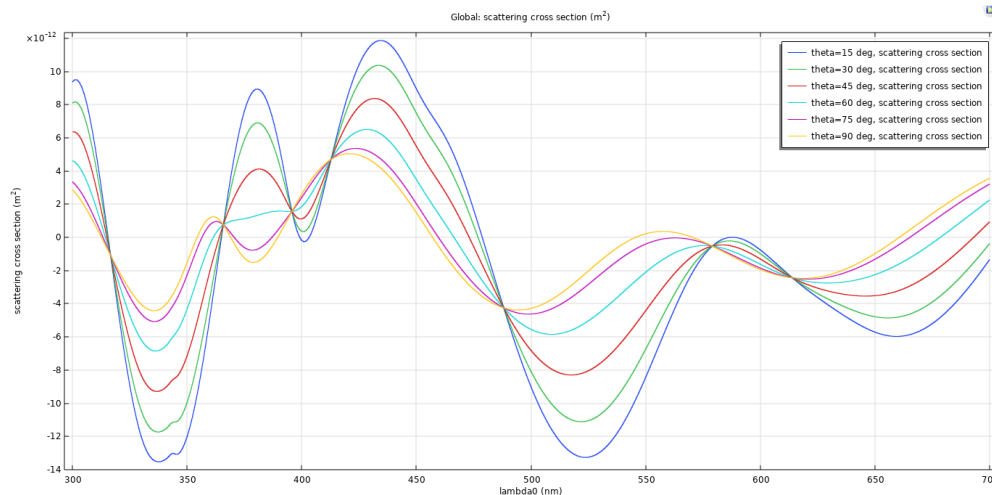
We Can Observe the Radiation Pattern Of 1\*5 Array of Nanoantenna Element with Spacing Of 200nm, From 300nm -700nm Wavelengths. We Can Observe the Scattering Amplitude Of  $10^{-6}$ V/m.

### 4.3.3 Effect of Change in Angle of Incidence of Wave Propagation on Scattering and Radiation Pattern

We varied different angle of incidences which are propagated on the 1\*5 Array of nanoantenna by suing parametric sweep function in the study. We have given theta as angle of incidence in parameters and simulated using parametric sweep and extracted results

**Figure 4.13**

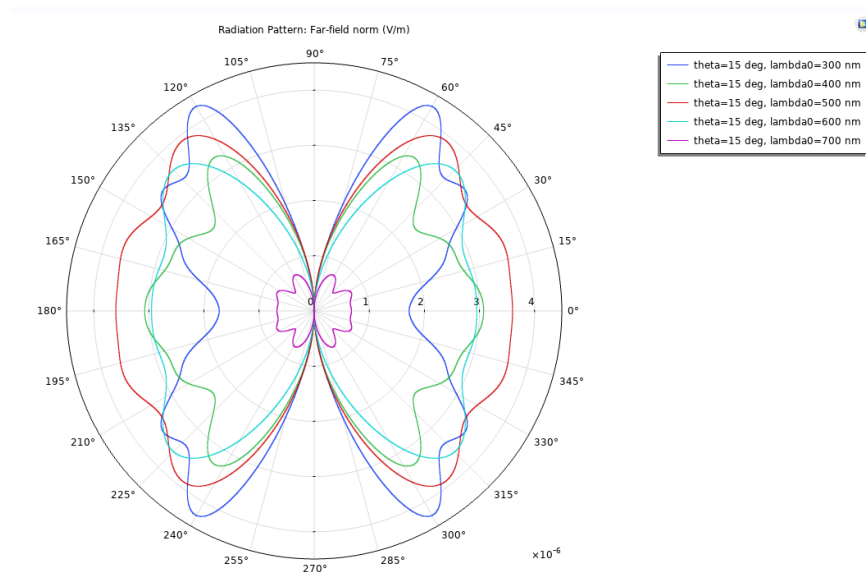
*Scattering Cross Section Of 1\*5 Array of Nanoantenna Element with Different Angle of Incidences*



We can observe the characteristic resonance of the 1\*5 array of nanoantenna with spacing of 100nm with different angle of incidences  $\theta = 15^\circ, 30^\circ, 45^\circ, 60^\circ, 75^\circ, 90^\circ$ . For all the angles we can observe the maximum peak at 430nm – 440nm wavelength range but the scattering value decreasing when we increase the angle of incidence.

**Figure 4.14**

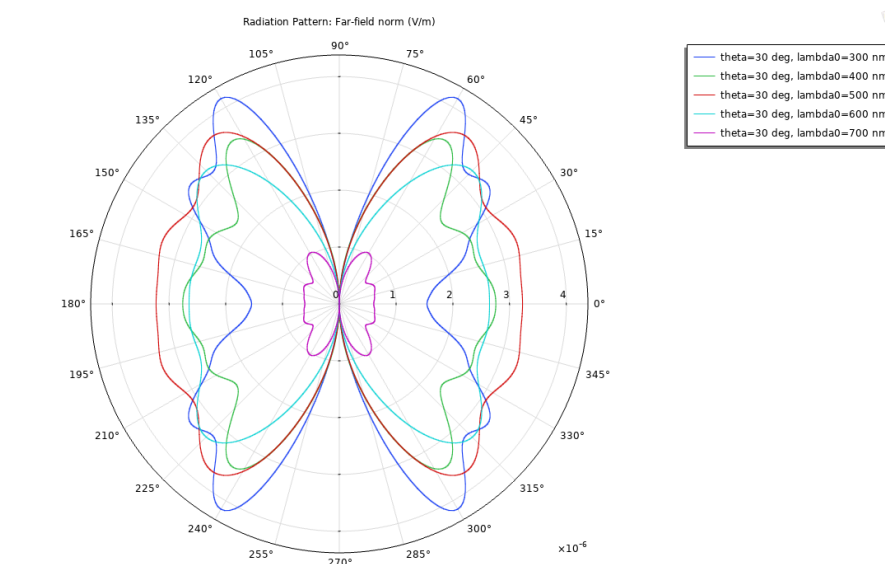
*Far Field Radiation Pattern of 1\*5 Array with Angle of Incidence,  $\theta=15^\circ$*



We Can Observe the Radiation Pattern Of 1\*5 Array of Nanoantenna Element with Spacing of 100nm With Angle of Incidence  $\theta = 15^\circ$ , From 300nm -700nm Wavelengths. We Can Observe the Scattering Amplitude Of  $10^{-6} \text{ V/m}$ .

**Figure 4.15**

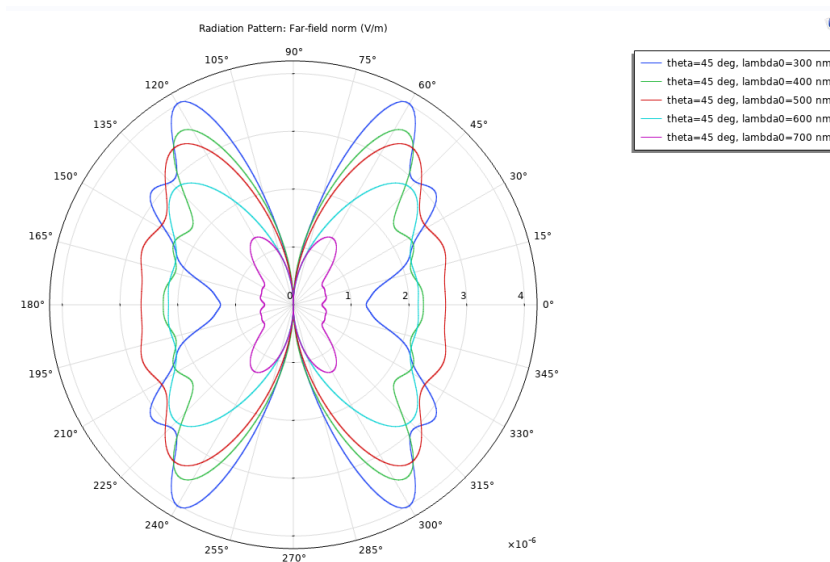
*Far Field Radiation Pattern of 1\*5 Array with Angle of Incidence,  $\theta=30^\circ$*



We can observe the radiation pattern of 1\*5 array of nanoantenna element with spacing of 100nm with angle of incidence  $\theta = 30^\circ$ , from 300nm -700nm wavelengths. We can observe the scattering amplitude of  $10^{-6}$ V/m.

**Figure 4.16**

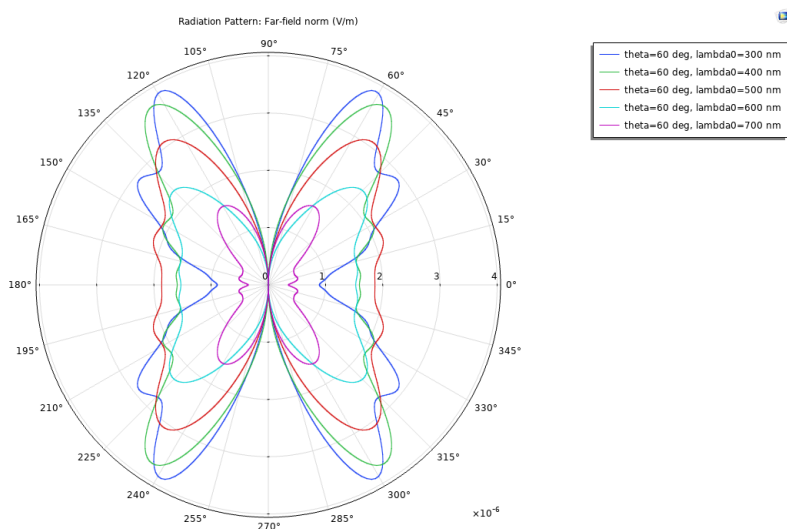
*Far Field Radiation Pattern of 1\*5 Array with Angle of Incidence,  $\theta = 45^\circ$*



We can observe the radiation pattern of 1\*5 array of nanoantenna element with spacing of 100nm with angle of incidence  $\theta = 45^\circ$ , from 300nm -700nm wavelengths. We can observe the scattering amplitude of  $10^{-6}$ V/m.

**Figure 4.17**

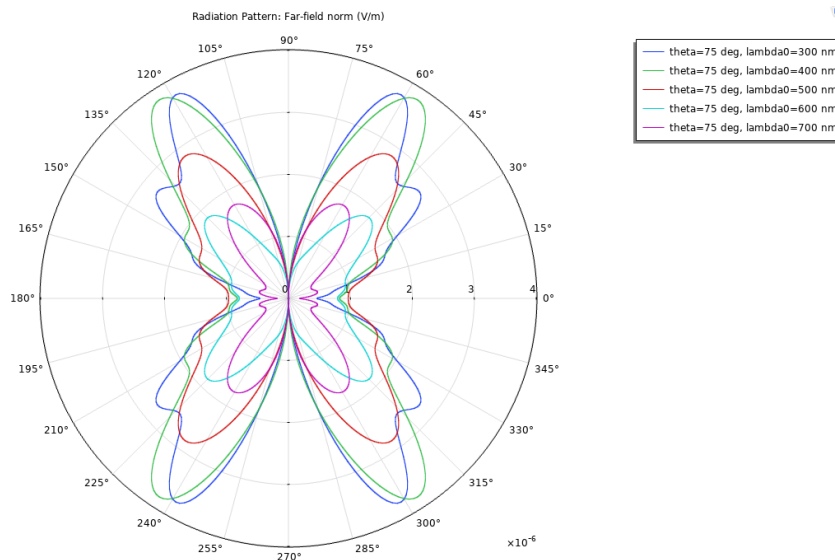
*Far Field Radiation Pattern of 1\*5 Array with Angle of Incidence,  $\theta = 60^\circ$*



We can observe the radiation pattern of 1\*5 array of nanoantenna element with spacing of 100nm with angle of incidence  $\theta = 60^\circ$ , from 300nm -700nm wavelengths. We can observe the scattering amplitude of  $10^{-6}$ V/m.

**Figure 4.18**

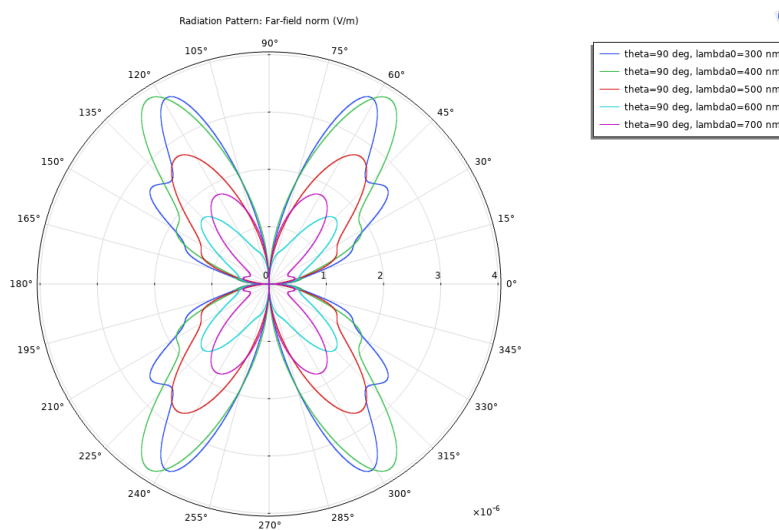
*Far Field Radiation Pattern of 1\*5 Array with Angle of Incidence,  $\theta = 75^\circ$*



We can observe the radiation pattern of 1\*5 array of nanoantenna element with spacing of 100nm with angle of incidence  $\theta = 75^\circ$ , from 300nm -700nm wavelengths. We can observe the scattering amplitude of  $10^{-6}$ V/m.

**Figure 4.19**

*Far Field Radiation Pattern of 1\*5 Array with Angle of Incidence,  $\theta = 90^\circ$*





We can observe the radiation pattern of  $1 \times 5$  array of nanoantenna element with spacing of 100nm with angle of incidence  $\theta = 90^\circ$ , from 300nm -700nm wavelengths. We can observe the scattering amplitude of  $10^{-6}$ V/m.

We can observe the change in the radiation plots when the angle of incidence  $\theta$  changes.

## **CHAPTER 5**

### **CONCLUSION AND RECOMMENDATIONS**

In summary, we started to design and simulate with a single optical nanoantenna and illustrated how it interacts with light for given material and geometry. In our investigation, we observed that single nanoantenna element upon exciting the light exhibits strong field scattering and directivity. Changing the geometry and Angle of incidence ( $\theta$ ) strongly influence the scattering resonance of the wavelength.

Furtherly, the single optical nanoantenna elements are extended into an array and shown how it interacts with light. We observed that, by increasing the number of nanoantenna elements increases the scattering of the light and enhances the directivity of the light. We therefore displayed the unique properties of dielectric nanoantenna elements which exhibits high scattering in short bandwidth when interacted with light.

As the future recommendations, the design can be built in a 3-D printer and by using practical approach of exhibiting the light which may give good results. The nanoantenna elements can be placed on glass or any other opaque materials which might provide better configuration for maximum transmission.

## REFERENCES

- Al, A., & Engheta, N. (2008). Tuning the scattering response of optical nanoantennas with nanocircuit loads. *Nature Photonics*, 2(5), 307–310.  
<https://doi.org/10.1038/nphoton.2008.53>
- Alda, J., Rico-García, J. M., López-Alonso, J. M., & Boreman, G. (2005). Optical antennas for nano-photonics applications. *Nanotechnology*, 16(5).  
<https://doi.org/10.1088/0957-4484/16/5/017>
- Asapu, R., Verbruggen, S., Claes, N., Bals, S., Denys, S., & Leuners, S. (2016). *FEM And Near-field Simulations : A Vital Mechanistic Tool for Studying Silver-based Plasmonic Systems Silver Plasmonic Systems : What and Where ?* 1–11.
- Balanis, C. A. (2005). *Antenna Theory: Analysis and Design, 3rd Edition*.  
<http://www.amazon.com/Antenna-Theory-Analysis-Design-Edition/dp/047166782X>
- Bashirpour, M., Forouzmehr, M., Hosseinienejad, S. E., Kolahehdouz, M., & Neshat, M. (2019). Improvement of Terahertz Photoconductive Antenna using Optical Antenna Array of ZnO Nanorods. *Scientific Reports*, 9(1), 1–8.  
<https://doi.org/10.1038/s41598-019-38820-3>
- Beheshti Asl, A., Rostami, A., & Amiri, I. S. (2019). Radiation pattern direction control in nano-antenna (tunable nano-antenna). *Optical and Quantum Electronics*, 51(11), 1–13. <https://doi.org/10.1007/s11082-019-2085-4>
- Bohren. (n.d.). *Aspects of light Atoms and fields*. 104.
- Codreanu, I., & Boreman, G. D. (2002). Integration of microbolometers with infrared microstrip antennas. *Infrared Physics and Technology*, 43(6), 335–344.  
[https://doi.org/10.1016/S1350-4495\(02\)00123-8](https://doi.org/10.1016/S1350-4495(02)00123-8)
- Comsol. (2013). *The Wave Optics Module User's Guide*.
- Djalalian-assl, A., Goh, X. M., Roberts, A., & Davis, T. J. (2011). *Optical Nano-*

*antennas*. September, 2127–2129.

- Filonov, D. S., Krasnok, A. E., Slobzhanyuk, A. P., Kapitanova, P. V., Nenasheva, E. A., Kivshar, Y. S., & Belov, P. A. (2012). Experimental verification of the concept of all-dielectric nanoantennas. *Applied Physics Letters*, *100*(20). <https://doi.org/10.1063/1.4719209>
- González, F. J., Gritz, M. A., Fumeaux, C., & Boreman, G. D. (2002). Two dimensional array of antenna-coupled microbolometers. *International Journal of Infrared and Millimeter Waves*, *23*(5), 785–797. <https://doi.org/10.1023/A:1015722821951>
- Ichimaru, S. (2019). Scattering of Electromagnetic Waves. *Statistical Physics of Dense Plasmas*, *1*, 39–52. <https://doi.org/10.1201/9780429431210-3>
- Kausar, A. S. M. Z., Reza, A. W., Latef, T. A., Ullah, M. H., & Karim, M. E. (2015). Optical nano antennas: State of the art, scope and challenges as a biosensor along with human exposure to nano-toxicology. *Sensors (Switzerland)*, *15*(4), 8787–8831. <https://doi.org/10.3390/s150408787>
- Krasnok, A E, Maksymov, I. S., Denisyuk, A. I., Belov, P. A., Miroshnichenko, A. E., Simovski, C. R., & Kivshar, Y. S. (2013). Optical nanoantennas. *Physics-Uspekhi*, *56*(6), 539–564. <https://doi.org/10.3367/ufne.0183.201306a.0561>
- Krasnok, Alexander E., Miroshnichenko, A. E., Belov, P. A., & Kivshar, Y. S. (2012). All-dielectric optical nanoantennas. *AIP Conference Proceedings*, *1475*(1), 22–24. <https://doi.org/10.1063/1.4750083>
- Large, N., Abb, M., Aizpurua, J., & Muskens, O. L. (2010). Photoconductively loaded plasmonic nanoantenna as building block for ultracompact optical switches. *Nano Letters*, *10*(5), 1741–1746. <https://doi.org/10.1021/nl1001636>
- Lezec, H. J., Degiron, A., Devaux, E., Linke, R. A., Martin-Moreno, L., Garcia-Vidal, F. J., & Ebbesen, T. W. (2002). Beaming light from a subwavelength aperture. *Science*, *297*(5582), 820–822. <https://doi.org/10.1126/science.1071895>
- Liu, Z., Boltasseva, A., Pedersen, R. H., Bakker, R., Kildishev, A. V., Drachev, V. P.,

- & Shalaev, V. M. (2008). Plasmonic nanoantenna arrays for the visible. *Metamaterials*, 2(1), 45–51. <https://doi.org/10.1016/j.metmat.2008.03.001>
- Liu, Z., Ni, X., & Kildishev, A. V. (2009). *Modeling Optical Nanoantenna Arrays with COMSOL Multiphysics*.
- Matsue, T. (2012). *Biosensing with plasmonic nanosensors*. 557(5), 8–10.
- Nojonen, E., & Turunen, J. (1994). Eigenmode method for electromagnetic synthesis of diffractive elements with three-dimensional profiles. *Journal of the Optical Society of America A*, 11(9), 2494. <https://doi.org/10.1364/josaa.11.002494>
- Noskov, R. E., Krasnok, A. E., & Kivshar, Y. S. (2012). Nonlinear metal-dielectric nanoantennas for light switching and routing. *New Journal of Physics*, 14. <https://doi.org/10.1088/1367-2630/14/9/093005>
- Novotny, L., & Van Hulst, N. (2011). Antennas for light. *Nature Photonics*, 5(2), 83–90. <https://doi.org/10.1038/nphoton.2010.237>
- Wessel, J. (1985). Surface-enhanced optical microscopy. *Journal of the Optical Society of America B*, 2(9), 1538. <https://doi.org/10.1364/josab.2.001538>